NASA CONTRACTOR REPORT 166304

An Engine Trade Study for a Supersonic STOVL Fighter/Attack Aircraft

Volume I - Trade Study Background and Methodology

B. B. Beard and W. H. Foley
General Dynamics Corporation

CONTRACT NAS2-10981
February 1982

NASA

NASA CONTRACTOR REPORT 166304

An Engine Trade Study for a Supersonic STOVL Fighter/Attack Aircraft

Volume I - Trade Study Background and Methodology

B. B. Beard and W. H. Foley
General Dynamics
Fort Worth Division
P. O. Box 748
Fort Worth, Tx 76101

Prepared for
Ames Research Center
under Contract NAS2-10981

NASA
National Aeronautics and Space Administration
Ames Research Center
Moffett Field, California 94035

This Page Intentionally Left Blank

FOREWORD

This Engine Trade Study for a Supersonic STOVL Fighter/Attack Aircraft was conducted under contract NAS2-10981, which was jointly sponsored by NASA Ames Research Center, (NASA/ARC), the Naval Air System Command (NAVAIR), and the David Taylor Naval Ship Research and Development Center (NSRDC). The contract monitor was Mr. D.G. Koenig of NASA/ARC. The study was conducted by General Dynamics' Fort Worth Division Aerodynamics and Propulsion Sections with Dr. W. H. Foley serving as program manager.

The authors wish to acknowledge the assistance provided by technical contacts W. P. Nelms, D. A. Durston, D. G. Koenig (of NASA/ARC), M.W. Brown (NAVAIR), and J. H. Nichols (NSRDC) and General Dynamics engineers C.W. Smith, A. E. Sheridan, H. L. Roland, D.C. Rapp, J. D. Pressley, and M. A. Kaiser. We also wish to acknowledge the gracious and timely assistance provided by the various engine manufacturers - Rolls Royce, General Electric, Pratt and Whitney, Detroit Diesel Allison, and Garrett AiResearch.

Dimensional quantities in this report are given in U. S. Customary Units. A table for conversion to the Système International d' Unités (SI) is provided in Appendix B.

Data proprietary to engine manufacturers and General Dynamics are supplied in Volume II of this report, for which distribution is limited to United States Government Agencies, and General Dynamics.

This Page Intentionally Left Blank

TABLE OF CONTENTS

TABLE OF CONTENTS (Cont'd)

LIST OF TABLES

LIST OF FIGURES

LIST OF FIGURES (Cont'd)

LIST OF SYMBOLS

Symbol	Meaning	Units
A_e	Ejector exhaust plane flow area	in^2
A_p	Ejector primary nozzle exit area	in^2
A_J	Engine core exhaust throat area ("jet area")	in^2
c	Wing mean chord	
c_{fg}	Nozzle gross thrust coefficient (actual/ideal thrust)	-
$C_{n\beta}$	Derivative of yawing moment coefficient with respect to angle of sideslip	deg^{-1}
C_p	Gas specific heat at constant pressure	ft-lbf/lbm °R
D	Ejector secondary air ram drag	lbf
D_1	Value of compressible flow function at Mach 1.0	.5317 lbm °R/lbf-sec
F_{Gi}	Ideal gross thrust	lbf
F_{pi}	Ejector primary nozzle ideal gross thrust	lbf
F_x	Axial component of ejector thrust	lbf
F_y	Vertical component of ejector thrust	lbf
g_c	Unit rationalizer	32.17 lbm ft/sec^2/lbf
H	$1/2\ (F_y/P_aA_e)\ ((\gamma-1)/\gamma)$	-
$I_{aircraft}$	Aircraft moment of inertia about axis of applied torque	lbm-ft^2
I_{high}	Moment of inertia, high pressure engine spool	lbm-ft^2
I_{low}	Moment of inertia, low pressure engine spool	lbm-ft^2
k	Mass split fraction, $\dot{m}_{aft}/\dot{m}_{fan}$	-
L_{engine}	Total angular momentum of engine spools	lbm-ft^2/sec
L_{high}	Angular momentum, high pressure engine spool	lbm-ft^2/sec

LIST OF SYMBOLS (Cont'd)

Symbol	Meaning	Units
L_{low}	Angular momentum, low pressure engine spool	lbm-ft^2/sec
$\dot{m}_{aft}$	Mass flow rate directed to aft nozzle	lbm/sec
$\dot{m}_{ch,min}$	Minimum choking mass flow rate	lbm/sec
$\dot{m}_e$	Mass flow rate at ejector exhaust	lbm/sec
$\dot{m}_{fan}$	Mass flow rate of engine bypass flow	lbm/sec
$\dot{m}_p$	Mass flow rate of ejector primary flow	lbm/sec
$\dot{m}_s$	Mass flow rate of ejector secondary flow	lbm/sec
M_o	Flight Mach number	-
$N_{ch,min}$	Minimum choking nozzle pressure ratio	-
P_a	Ambient pressure	psia
P_{S_e}	Static pressure at ejector exhaust plane	psia
P_{T_e}	Total pressure at ejector exhaust plane	psia
P_{T_p}	Total pressure at ejector primary nozzle exit	psia
$P_{T_{supply}}$	Total pressure of ejector primary flow supply	psia
q	Dynamic pressure	psia
R	Gas constant for air	53.35 ft-lbf/lbm °R
S	Wing area	ft^2
T_a	Ambient temperature	°R
T_{eng}	Uninstalled engine thrust	lbf
T^*_{eng}	Installed engine thrust	lbf
T_{S_e}	Static temperature at ejector exhaust plane	°R
T_{T_e}	Total temperature at ejector exhaust plane	°R
T_{Tp}	Total temperature of ejector primary airflow	°R
T_{T_s}	Total temperature of ejector secondary airflow	°R

LIST OF SYMBOLS (Cont'd)

Symbol	Meaning	Units
$T_{T_{supply}}$	Total temperature of ejector exhaust plane	°R
V_e	Flow velocity of ejector exhaust	ft/sec
V_x	Axial component of flow velocity at ejector exhaust	ft/sec
V_y	Vertical component of flow velocity at ejector exhaust	ft/sec
V_∞	Flight velocity	ft/sec
W_{corr}	Engine fan design corrected mass flow rate	lbm/sec
W_{eng}	Engine weight	lbf
w_{high}	Angular velocity of high pressure engine spool	sec^{-1}
w_{low}	Angular velocity of low pressure engine spool	sec^{-1}
α_R	Ejector ram drag parameter ($D-F_x/V_\infty\sqrt{F_y}$)	lbf/ft/sec
β	Angle of sideslip	deg
γ	Gas ratio of specific heats	-
η_a	Ejector axial momentum recovery (F_x/D)	-
λ	Uninstalled thrust split (bypass thrust/core thrust)	-
λ^*	Installed thrust split (ejector thrust/core thrust)	-
ρ_{S_e}	Gas density at ejector exit plane	lbm/ft^3
$\tau_{applied}$	External torque applied to airframe	$lbm/ft^2/sec^2$
ϕ	Ejector isentropic augmentation ratio	-
Ψ	Gyro-static coupling parameter	-

LIST OF ABBREVIATIONS (Cont'd)

Abbreviation	Meaning
AIROPS	Air Operations
ADEN	Augmented Deflecting Exhaust Nozzle
APU	Auxiliary Power Unit
ARC	Ames Reasearch Center
BPR	Bypass Ratio
CPR	Compressor Pressure Ratio
DFE	Derivative Fighter Engine
FPR	Fan Pressure Ratio
NAVAIR	Naval Air Systems Command
NPR	Nozzle Pressure Ratio
NSRDC	Naval Ship Research and Development Center
PCB	Plenum Chamber Burning
RALS	Remote Augmentor Lift System
RCS	Reaction Control System
STOVL	Short Takeoff, Vertical Landing
TIT	Turbine Inlet Temperature
VEO WING	Vectored Engine Over Wing
V/STOL	Vertical/Short Takeoff and Landing

1. INTRODUCTION

Early in 1980 General Dynamics began a program to investigate the possibility of designing a V/STOL fighter/attack aircraft incorporating an existing engine, as opposed to the conventional process of designing conceptual aircraft to given missions, which generally require new engines. The logic behind this was two-fold: such a demonstrator aircraft could be built much faster and cheaper than one requiring an engine development. This report documents the search for an optimum engine candidate for an E-X flight demonstrator configuration, as described below.

1.1 Propulsion Concept

One of the propulsion systems that appeared attractive was the ejector system developed by DeHavilland under contract to NASA Ames Research Center and the Canadian Department of National Defense (References 1 through 4). This ejector system has a well-established data base and was tested at Ames on a large scale J97 powered model. A summary of this test program is presented in Reference 6.

From the perspective of General Dynamics, the advantage of an ejector system is not just its high augmentation. It is more significant that the ejector exhaust is cool and its velocity is relatively low. Although afterburning systems such as RALS and PCB are capable of equally good augmentations, and although lift engines are probably the most compact systems available, it is our opinion that the environmental and inlet injestion problems associated with the extremely hot and high-velocity exhausts of these other systems have not been fully addressed. Our own investigations indicate that it is not only possible to get into very real problems when operating aircraft based on such systems, but highly probable. Although fixes, such as deck grids, might be found, it seems certain that such fixes will limit the operational usefulness of hot-footprint aircraft. An ejector system simply avoids the problem.

To be sure, an ejector system does present some difficulties, the largest single one being the ram drag of the entrained air at forward speeds. In fact, the original ejector model tested at the Ames 40- by 80-foot wind tunnel was quite marginal in its ability to transition from ejector-borne to wing-borne flight due to ram drag (Reference 2). Although it was demonstrated that this could be overcome by vectoring the ejector nozzles aft, an operational aircraft would require controllable vector angles that in turn would require quite complex actuation systems. One way to avoid this problem is to duct only part of the engine flow to the ejector and to exhaust the rest to a single, vectorable nozzle. Further, if only fan air is used to power the ejector, the problem of ducting hot gases is eliminated. Therefore, for the E-X propulsive system, the fan air flow powers a set of ejectors forward on the aircraft, while the core air is ducted and vectored separately aft. This concept, with fan and core air separated, is shown schematically in Figure 1-1.

Figure 1-2 shows the propulsive configuration during hovering flight, while Figure 1-3 shows the transition or STO regime, and Figure 1-4 shows up-and-away flight. (These three figures show the present system as drawn around a General Electric engine. The earlier concepts, which were drawn around Pegasus-type engines, differ slightly.)

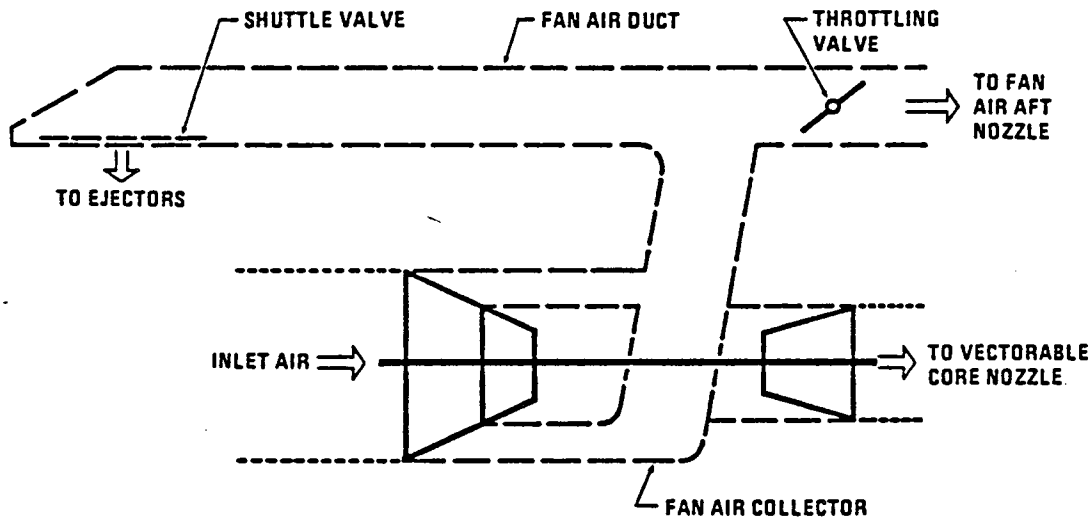

Figure 1-1 Propulsive System Schematic

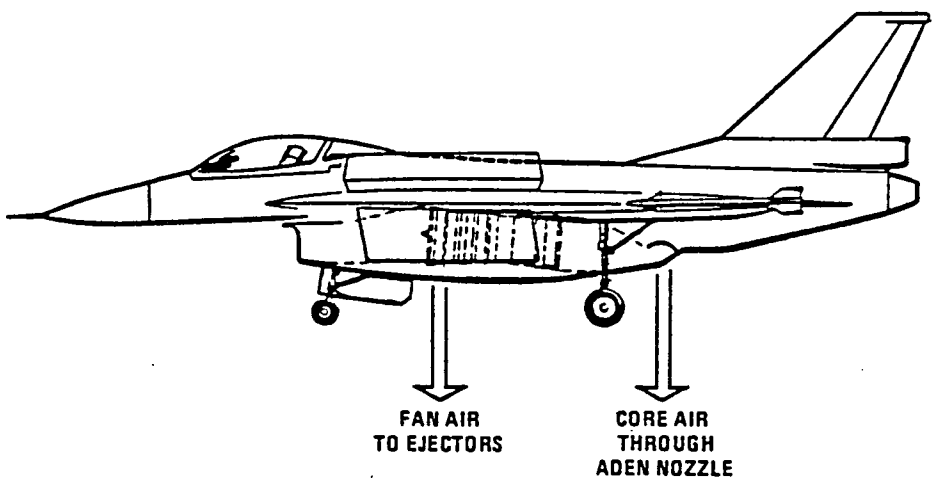

Figure 1-2 Propulsion System — Hover Configuration

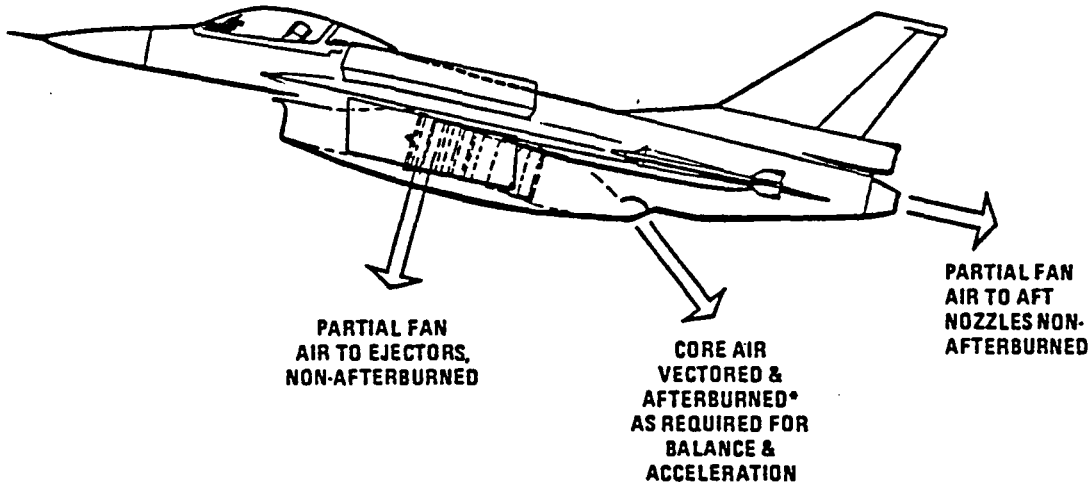

**CORE AFTERBURNED ONLY ON F101-DFE CONFIGURATIONS*

Figure 1-3 Propulsion System — STO and Transition Configuration

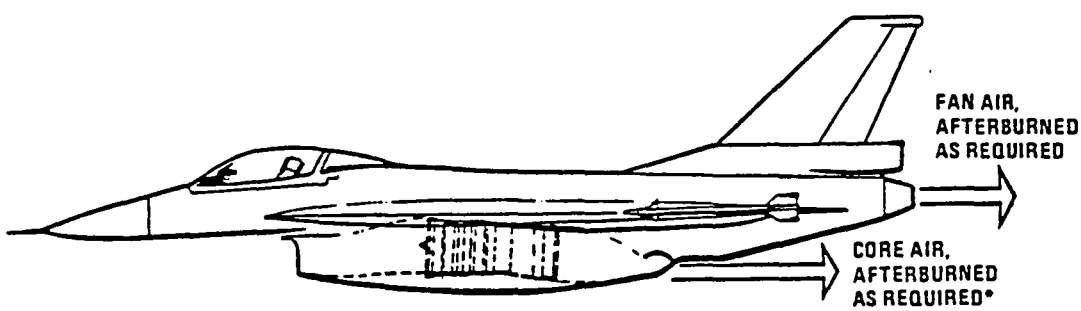

**ONLY ON F101-DFE CONFIGURATIONS*

Figure 1-4 Propulsion System — Up-and-Away Configuration

1.1.1 Operational Assumptions

The ultimate operational aircraft envisioned will have a mid-1990's Initial Operating Capability. It is not clear what naval requirements will be at that date, so the following assumptions have been made:

A. In 1995 the Navy will be using large-decked carriers like those presently in use. While dispersive requirements may lead the Navy to smaller decks in the early 21st century, it is unlikely that the carriers in that time frame will be much smaller than the Essex class, i.e., 600 ft decks.

B. A naval aircraft in the 15,000 to 30,000 lb class is too small a weapons platform to perform primary fleet air defense or deep interdiction missions. It would be more appropriate to assign to it close air defense and close air support.

The first assumption above has led General Dynamics to consider only STOVL concepts. We use the term STOVL to mean that in a military mission sense, the only way takeoff can be achieved is through a STO deck run of roughly 400 feet. Vertical landing capability is defined as coming aboard with a reasonable fuel reserve plus any expensive weapons which might be unexpended.

By this definition STOVL accomplishes the prime benefit of VSTOL by greatly increasing AIROPS flexibility and decreasing deck cycle times while, at the same time, removing catapult and arresting gear machinery and support personnel from the carrier.

The second assumption has led General Dynamics to pick a modified Type Specification 169 (TS 169) as the design goal. While it is not yet known to be fully responsive to the needs post-1995 Navy, it nonetheless describes the characteristics of a vehicle designed to perform viable military missions and, thus, provides a good starting baseline. A thorough discussion of our modifications to TS 169 is provided in Reference 5, the final report for the E-X aerodynamic technology study.

1.2 Pegasus Powered Configurations

The initial designs of the E-series were drawn around the Rolls-Royce 11F-35 engine, for a flight demonstrator, and a Rolls-Royce J-engine, for the operational aircraft. The 11F-35 fan is presently being tested at Rolls-Royce. The J-engine is still in the conceptual design stage. In the Rolls-powered configurations, the core flows are not afterburned for the operational aircraft.

1.2.1 Configuration E-1

The first configuration in the series attempted to incorporate the ejector with a VEO-wing . In this design, fan air exhausted over two VEO nozzles when it was not ducted to the ejector. While this may have produced an outstanding STO aircraft, structural design difficulties developed between the wing box and the fan air duct. Thus, this design was refined to avoid the problem.

1.2.2 Configuration E-2

In this configuration (Figure 1-5), the ejectors were placed in oversized, F-16 type strakes. The aft fan air exhaust was ducted to a 2-D, afterburning nozzle, and the core flow exhausted to a vectorable, axisymmetric nozzle. Initial performance indicated that

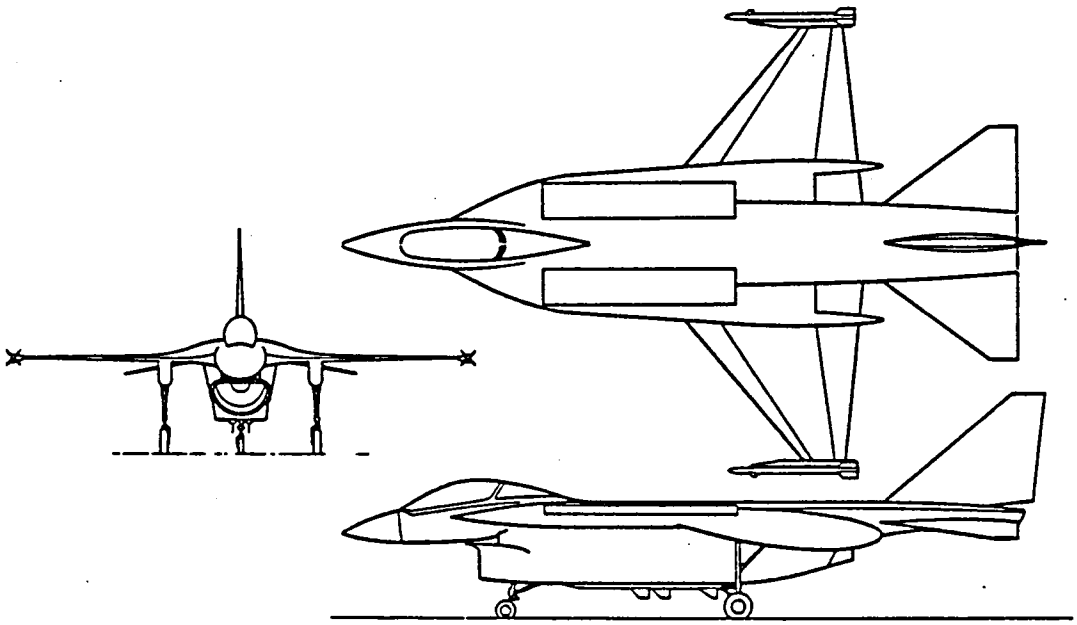

Figure 1-5 Configuration E-2

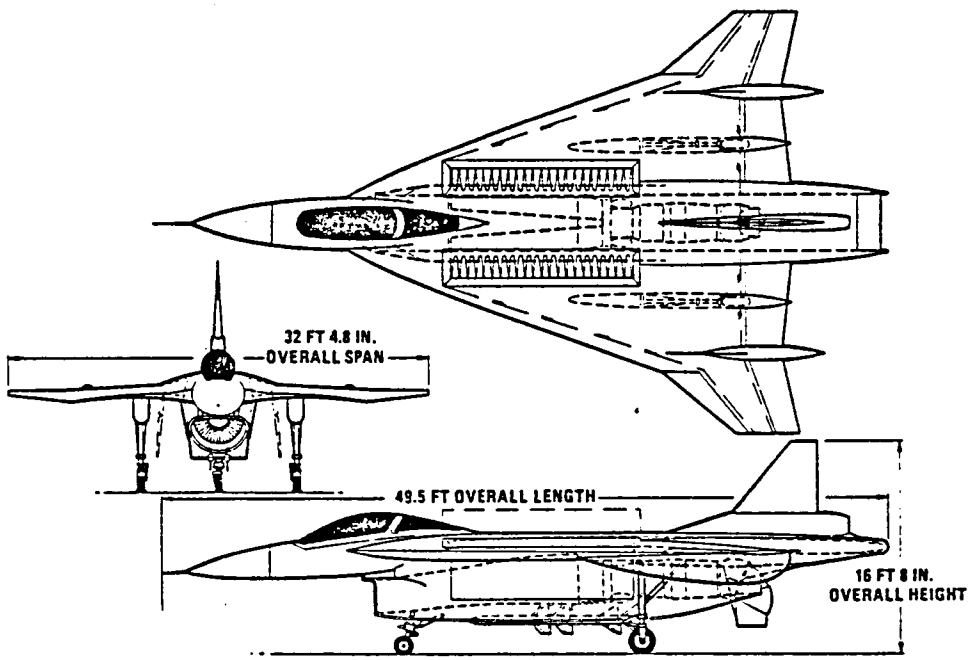

Figure 1-6 Rolls Royce Powered Configuration E-3

the aircraft could meet most of TS 169 with the exception of point performance. Because of structural interference between the ejectors and the wing box, the wing had to be located aft in a non-optimum position. The resultant impact on the area curve and trim drag was such that the configuration was capable of only subsonic flight. In order to increase the flexibility of locating the ejector relative to the c.g., and the wing with respect to the c.g. and the area curve, a long-root-chord configuration (whose diffuse structure allowed such flexibility) was investigated.

1.2.3 Configurations E-3 through E-7

An F-16XL cranked-arrow wing was placed around the E-2 fuselage and propulsion system to become Configuration E-3 (Figure 1-6). Preliminary analysis indicated that, with full-span leading edge devices for maneuver, this J-engine configuration would meet TS 169 escort mission and point performance, while, with the 11F-35 engine, a good flight demonstrator could be achieved.

A further refinement of E-3 was attempted in configuration E-4 - the aft fan air nozzle was eliminated and the fan air was remixed with the core air through an ADEN nozzle when not being used in the ejectors (Figure 1-7). However, this required that the fan and core pressures be matched. This sufficiently degraded the performance of the Pegasus-type engine that further development of E-4 was stopped and E-3 became the standard for further development of the series.

At this stage in the development it became questionable that the 11F-35 would be funded for development. Although the 11F-35 engine would be sufficient for powering an E-3 flight demonstrator, it appeared very unlikely that the engine would be satisfactory for an operational E-3 aircraft. Therefore, under the present study a search for an alternate engine was initiated. The General Electric F101 DFE emerged as a suitable candidate, and became the baseline powerplant for an aerodynamic technology study under NASA contract NAS2-11000. In the final report of that study (Reference 5), configurations E-5 through E-7 are discussed in detail. The E-3 propulsion system is used in those configurations, which merely involve planform changes. The term "E-X" is used to describe the general set of configurations which employ this propulsion system. (Configurations E-3/DFE through E-6 are shown in Figures 1-8 through 1-10. Figure 1-11 is a three-view of the E-7 configuration).

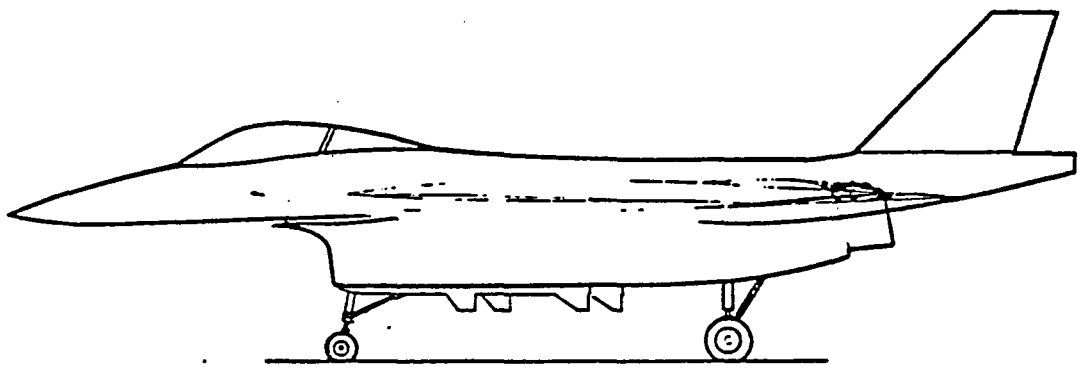

Figure 1-7 Configuration E-4

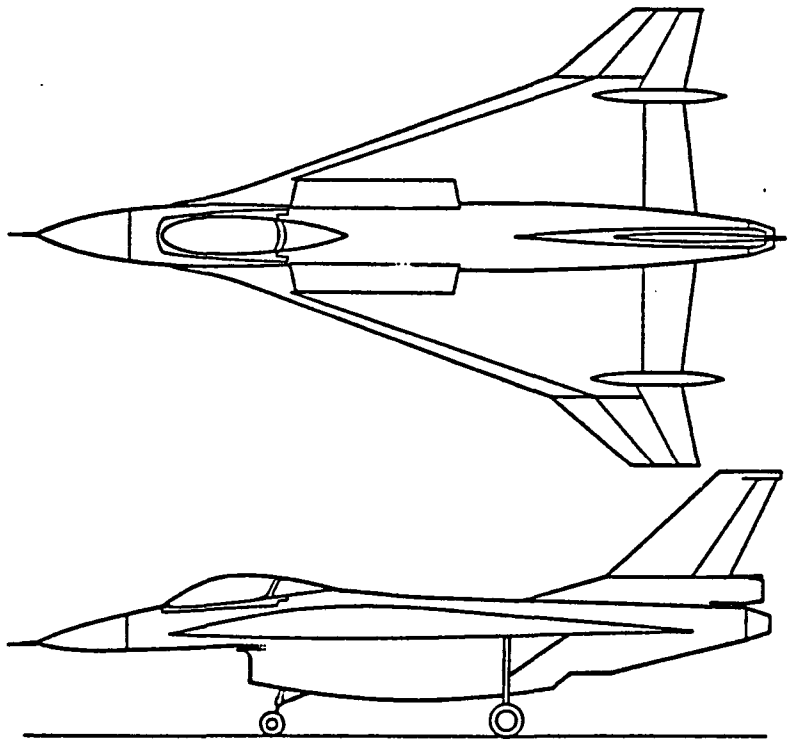

Figure 1-8 Configuration E-3/DFE

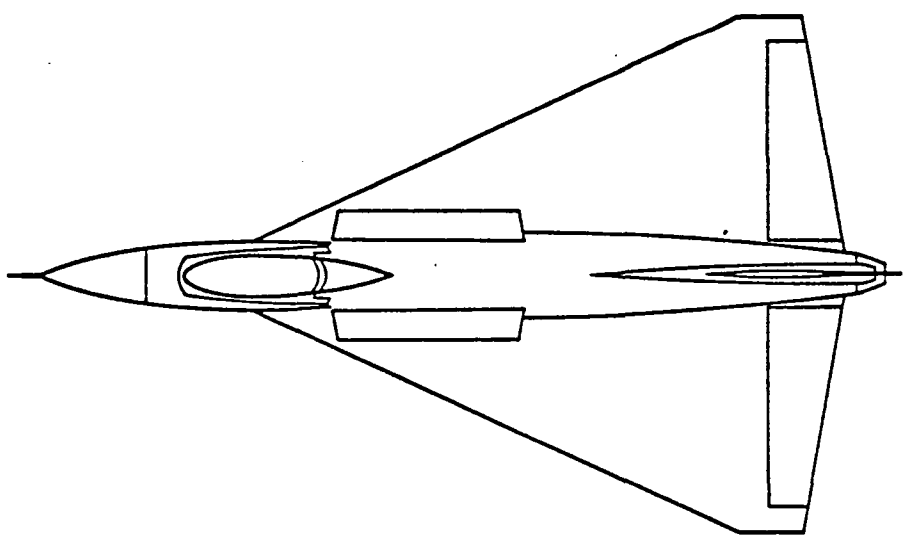

Figure 1-9 Configuration E-5

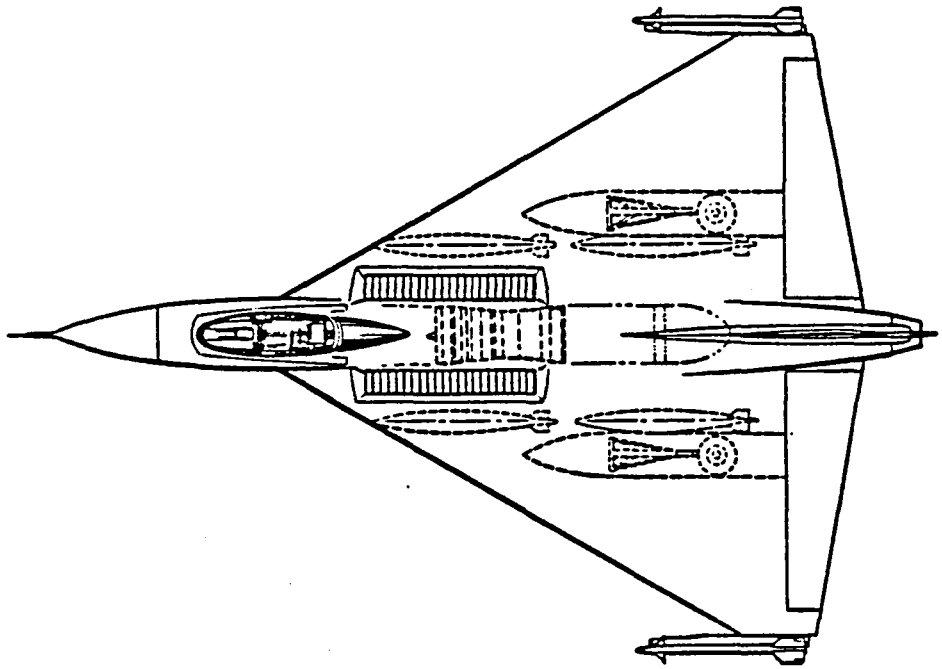

Figure 1-10 Configuration E-6

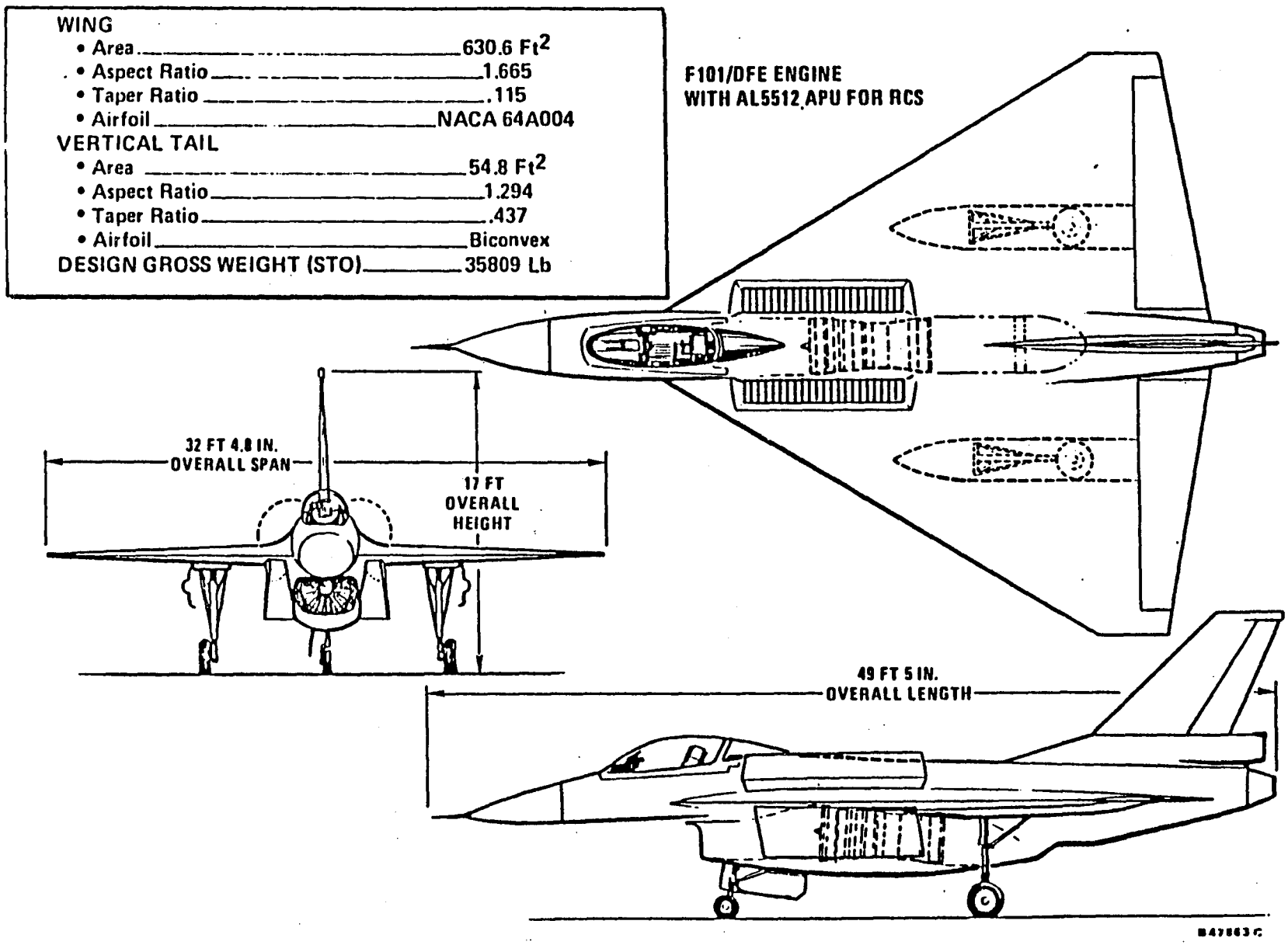

Figure 1-11 Three-View of Configuration E-7

2. GENERAL REQUIREMENTS

The E-X propulsion system concept requires a turbofan engine, which will be operated in a separated flow or two-stream mode. The intent of the Engine Trade Study was to explore configurations which would involve only recasing and minor control system changes for existing engines, and which would involve no major internal gaspath changes beyond those necessary to adapt the engine to the E-X configuration.

The size and weight dependence of the ejectors and ducting, as well as thrust sensitivity to pressure losses, place a premium on having a fan pressure ratio that is moderately high, and certainly above 2.

The above considerations alone are sufficient to screen a large number of engines from further analysis. In particular, all turbojet engines and all single stage fan turbofan engines can be eliminated from candidacy.

Together with modest limitations on thrust size, the field was narrowed to 6 primary engine candidates. These six engines are listed in Table 2-1, together with some key parameters. Note that three of the engines in the table can only be identified here by numerical tags, since the data contained here are proprietary, and in some cases are confidential, if associated with a specific engine.

Basic engine cycle data were derived from engine manufacturers' computer decks acquired by General Dynamics. Identified in the table are thrust level, fan/core-thrust split, bypass ratio, and fan pressure ratio at sea level/static/tropical day/hover conditions in E-X installation. The next section describes the installation calculations in greater detail.

	(SLS/INSTALLED THRUST)	THRUST SPLIT	BPR	FPR
F101-GE-100	20479	1.87:1	1.93	2.27
ENGINE 18	24661	1.54:1	1.15	2.45
F101 DFE	18117	.83:1	.78	3.16
TF 41	14051	.79:1	.75	2.32
ENGINE 4	18002	.65:1	.58	2.98
ENGINE 16	10244	.48:1	.41	3.23

B49394

TABLE 2-1 KEY PARAMETERS FOR STUDY ENGINES

3. TRADE STUDY METHODOLOGY

After the initial screening process, design data were generated for each of the candidate engines. The data included a maximum airflow for inlet sizing, as well as thrust level and thrust split at a design point in order to establish ejector and core nozzle positions relative to the aircraft center of gravity.

A preliminary aircraft layout of the E-3 with the Rolls-Royce 11F-35 had been made prior to the trade study. Using the generated design data, the E-3 configuration was laid out around several of the other candidate engines.

Based on the experience gained from the layouts and subsequent analysis, the candidate engines were compared for suitability for E-3, and the most suitable engine, the General Electric F101 DFE, was selected for further study.

3.1 Design Data

The design point for which data were generated was sea level, static, tropical day, and military power. F-16 type bleed and horsepower extractions were used.

The inlet was assumed to be an F-16 type normal shock inlet with fixed geometry. The throat area was sized for an up and away maximum corrected airflow. Blow-in door area was assigned to provide an inlet pressure recovery of .965 at the design point hover conditions.

The core nozzle was assumed to be an ADEN/MADEN type vectorable nozzle. A gross thrust coefficient C_{fg} of .96 was assumed in the 90° downward vectored configuration, which is typical for the ADEN.

The ejectors were of the Ames/DeHavilland type. The ejector isentropic augmentation ratio, ϕ (the ratio of actual to primary nozzle ideal thrust) was assumed to be 1.63. Variations of augmentation ratio with NPR, gas temperature, and forward velocity were not taken into account at this point.

Apart from the normal installation effects of inlets, ducts, nozzles, and extractions, the engine cycle itself was not modified. Instead the bypass duct entrance and core exit conditions were taken to represent actual flow properties of the bypass and core streams as installed in E-3. However, some modification of the engine cycle of the F101 DFE was assumed in the tailoring studies that followed the screening portion of the Engine Trade Study.

A table of the design parameters for the candidate engines is given in the proprietary volume of this report.

4. DEVELOPMENT OF EVALUATION CRITERIA

As the trade study progressed, it became apparent that the two most significant propulsive variables for the E-X study are the fan-to-core thrust split (λ) and the fan pressure ratio (FPR). The thrust split can be expressed as either an uninstalled thrust split λ or an installed thrust split λ^*. The FPR must be degraded by the inlet pressure recovery and ejector duct losses to derive the ejector primary nozzle pressure ratio.

These variables are significant because of their relation to ejector size and the relative spacing of the ejector and core nozzle. As the FPR increases, the ejectors become more compact at a given thrust level; if FPR is fixed, the ejectors grow larger as λ increases. The interaction of these two variables is best studied on a thrust split-fan pressure ratio plane.

In the E-X configuration, it is desirable to have both a high FPR and a reasonable λ, in order to keep ejector size reasonable and still derive maximum thrust benefit from the ejector augmentation. However, most of the candidate engines in the trade study are mixed flow turbofans. Such engines have a pressure matching condition at the turbine exit, which imposes a work extraction limitation on the core flow. The fan flow power requirement goes up with either increasing mass flow or increasing pressure ratio. Thus, a high FPR and a high λ are competing requirements in a mixed flow engine, although higher power densities in the core (i.e., bigger TIT's) allow better λ-FPR tradeoffs.

A graph showing the λ-FPR tradeoffs for the candidate engines is included in the proprietary volume of this report.

Limitations on thrust split and pressure ratio can be established for the E-X configuration (see Figure 4-1). A limit is placed on FPR at the high end, since ejector instability and separation may become a problem at primary nozzle NPR's above the range of 3.0 - 3.5. High thrust splits may be undesirable from the standpoint of transition performance, since ejector ram drag will become large relative to core thrust. Until the problem of transition can be decomposed parametrically, an upper limit of 1.3 has been placed on thrust split. A lower bound on thrust split can be derived by considering that minimal total thrust benefit is derived from the ejectors at low λ, thus driving up the uninstalled engine thrust requirement. Also, low FPR's result in large ejector size, with consequent problems in laying out the aircraft.

4.1 Afterbody Integration Problem

It was the low FPR constraint that first received analytical attention. It was during the layout of the E-3/F101-GE-100 aircraft that the problem with very low FPR propulsion systems became apparent.

For the particular combination of thrust split and pressure ratio provided by the F101-GE-100, the ejector size and location relative to the core nozzle are such that the core nozzle is forced to exhaust between the ejector rows. This circumstance raises a number of design problems. Compatibility with the inboard diffuser walls of the ejector forces the ADEN to a very high aspect ratio. Integrating the fuselage aft of the core nozzle with the diffuser walls and with the aft nozzle becomes impossible without encountering severe Coanda flow attachment and skin heating problems.

The condition for which the core nozzle shifts to a position forward of the aft end of the ejectors was quantified for "reasonable" parametric wing growth. "Reasonable" was

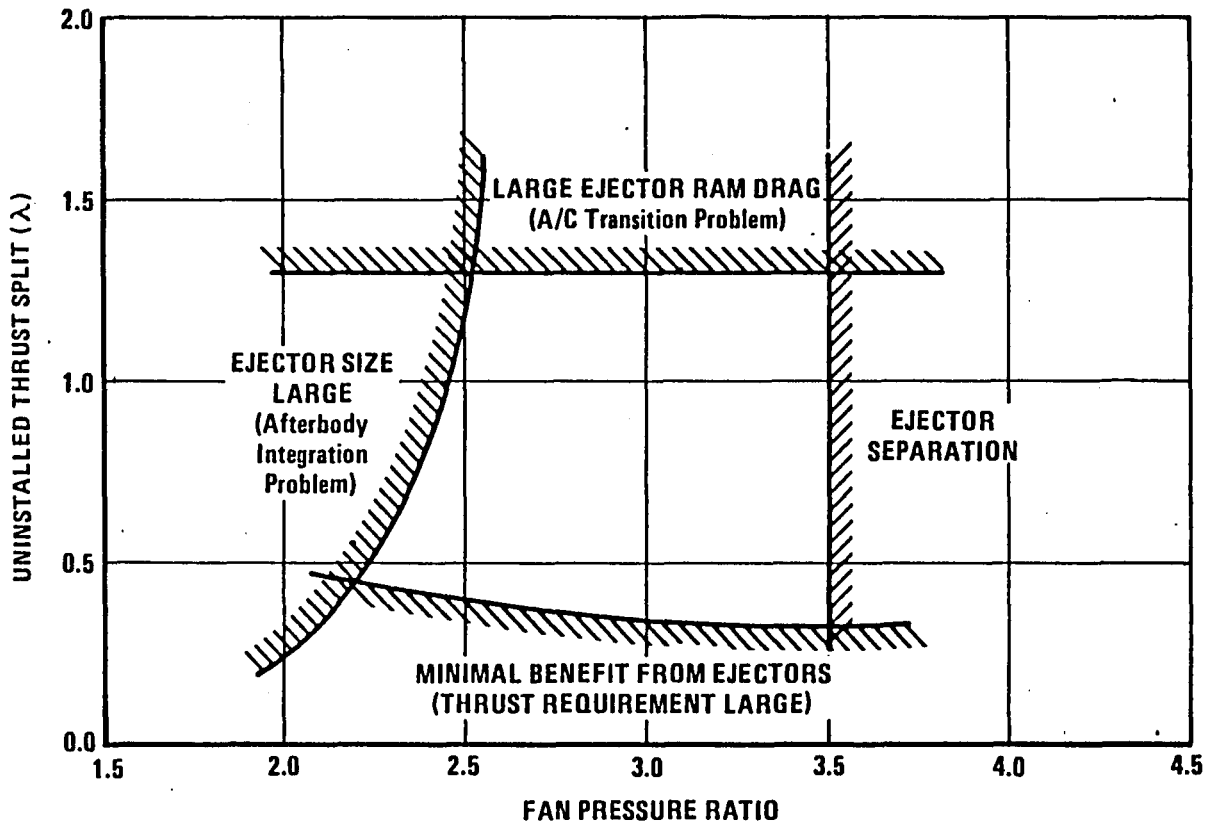

Figure 4-1 Limitations on Thrust Split and Fan Pressure Ratio

defined as wing area growing in proportion to installed thrust level, so that thrust level drops out of the parametrization (i.e., T^*_{eng}/S is constant - for this analysis, T^*_{eng}/S = 34.6 lbf/ft^2). The resulting curve in the λ-FPR plane is shown in Figure 4-2. (A similar figure, with data for some candidate engines plotted, is provided in the proprietary volume of this report.) As could be anticipated, the problem is more severe at higher thrust splits, for which the ejectors are larger.

4.2 Thrust-Weight Formalization

The above analysis, albeit enlightening, is not entirely satisfactory. The simplifying assumption of reasonable wing growth helps to make the problem tractable, but wing size and engine thrust level ought to be varied independently in any such parametric analysis.

A more general problem that needed to be introduced into the thrust split - fan pressure ratio analysis was the requirement for the level of installed engine thrust to exceed the aircraft zero fuel weight by a certain margin. The uninstalled engine thrust level required for hover at constant weight is itself a function of thrust split because it is only the bypass thrust which is augmented. Further, if the weight of the aircraft is allowed to vary as a function of FPR, λ, and engine thrust level, the engine thrust required for hover will also vary up or down with the weight. Engine thrust thus appears on both sides of the thrust-weight balance equation in this parametrization.

Figure 4-3 shows the result of such an analysis. The E-3/F101 DFE aircraft was taken as a baseline for weight, with individual component weights allowed to vary with FPR, λ, and engine thrust. Installed thrust was computed from uninstalled thrust and installation factors. The figure displays lines of constant minimum acceptable uninstalled engine thrust on a λ-FPR plane. Minimum acceptable thrust is defined as that uninstalled thrust that will result in an installed thrust equal to aircraft zero fuel weight plus a margin for fuel and a margin for reaction control system capability.

The intent of the thrust-weight formalization and the development of the λ-FPR minimum uninstalled thrust maps was to provide an analytical means of interfacing with engine manufacturers' performance estimates. The generalized variables of fan pressure ratio, uninstalled thrust, and uninstalled thrust split can be readily interpreted by engine manufacturers. Nominally, each point on the λ-FPR map represents a viable aircraft configuration at least from the standpoint of ejector and wing geometric compatibillity and of acceptable hovering thrust. Of course, the further the λ-FPR point from the E-3/DFE baseline point, the further the basic sizing assumptions are strained.

The graph reflects an assumption about wing growth that is tied to the afterbody integration problem. In the right hand portion of the plane, where the minimum thrust lines are nearly horizontal, the wing area is kept at the baseline level of the E-3/F101 DFE. However, for the lower fan pressure ratios, the wing is allowed to grow just enough to put the core nozzle at the aft end of the ejector rather than between the ejector rows. The figure shows lines of constant wing area. As can be seen, a severe penalty can be paid in thrust required at the lower FPR's.

Figure 4-4 is similar, except that it shows lines of constant aircraft zero fuel weight. This figure shows how most of the variation in minimum thrust is due more to the installation effect of thrust split than to the increase in gross weight.

Some general characteristics of these plots may be discerned. As pointed out above, there are two distinct regions of the graph, which involve different assumptions about wing and body growth. Region I, on the right-hand side of the plane, reflects a fixed wing

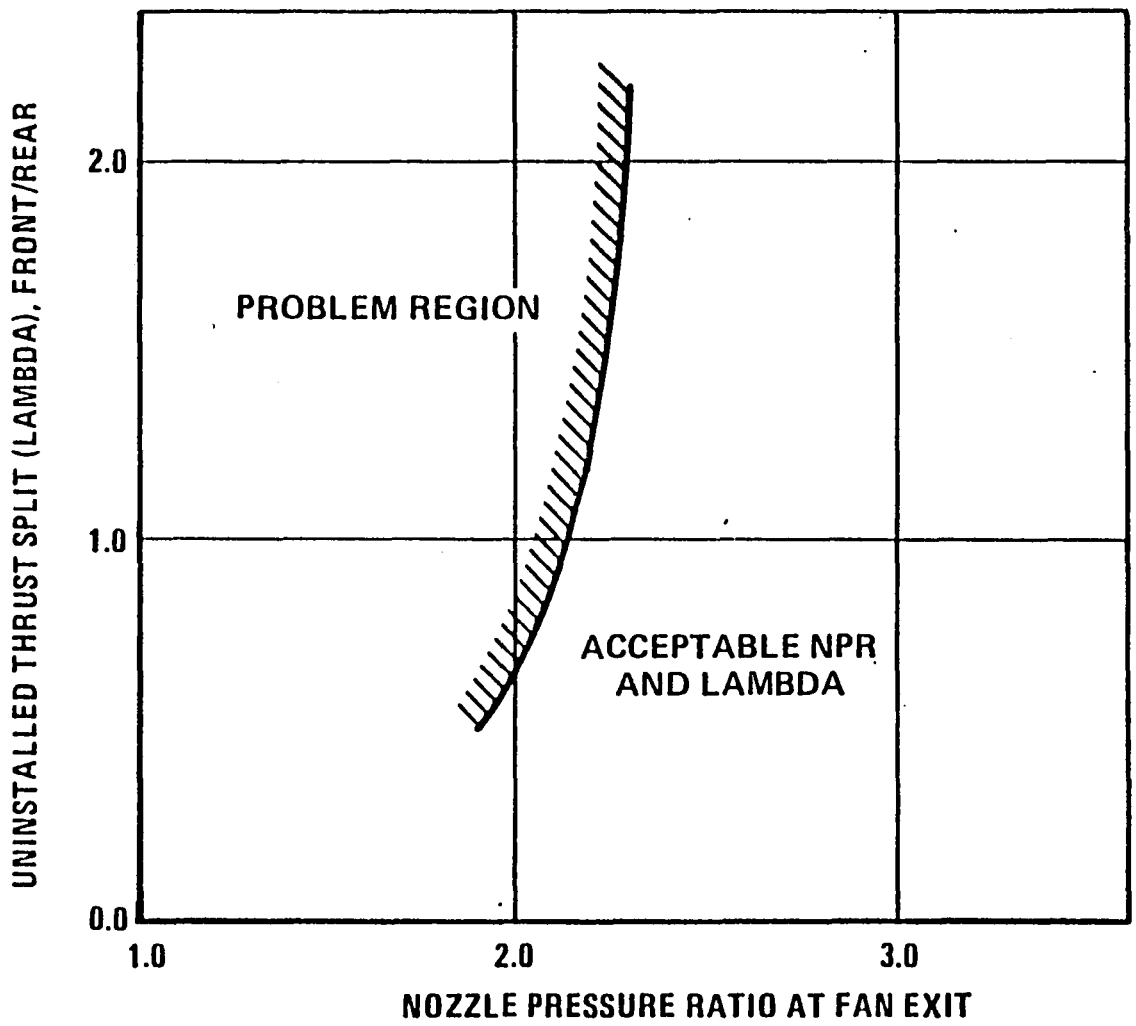

Figure 4-2 Critical Afterbody Integration Region

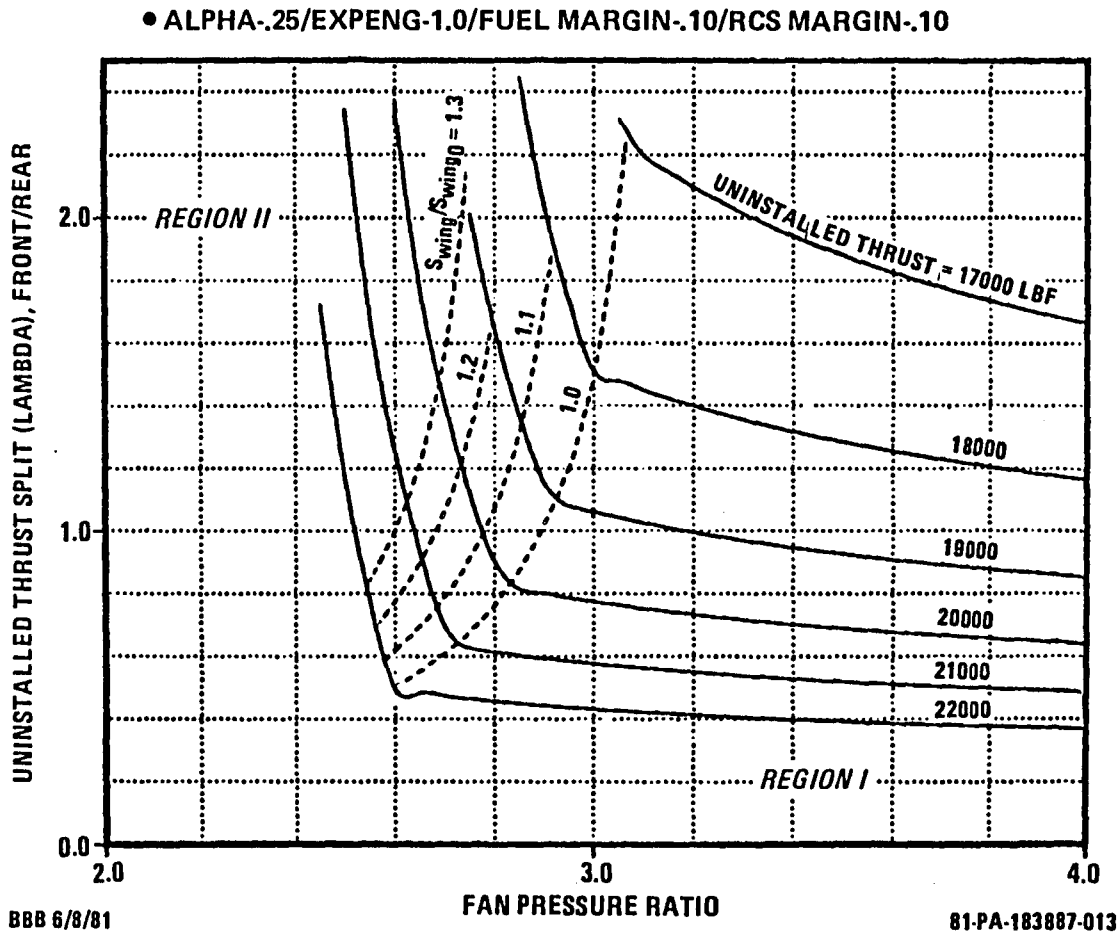

Figure 4-3 Minimum Uninstalled Engine Thrust Requirement (with Constant Wing Area Lines)

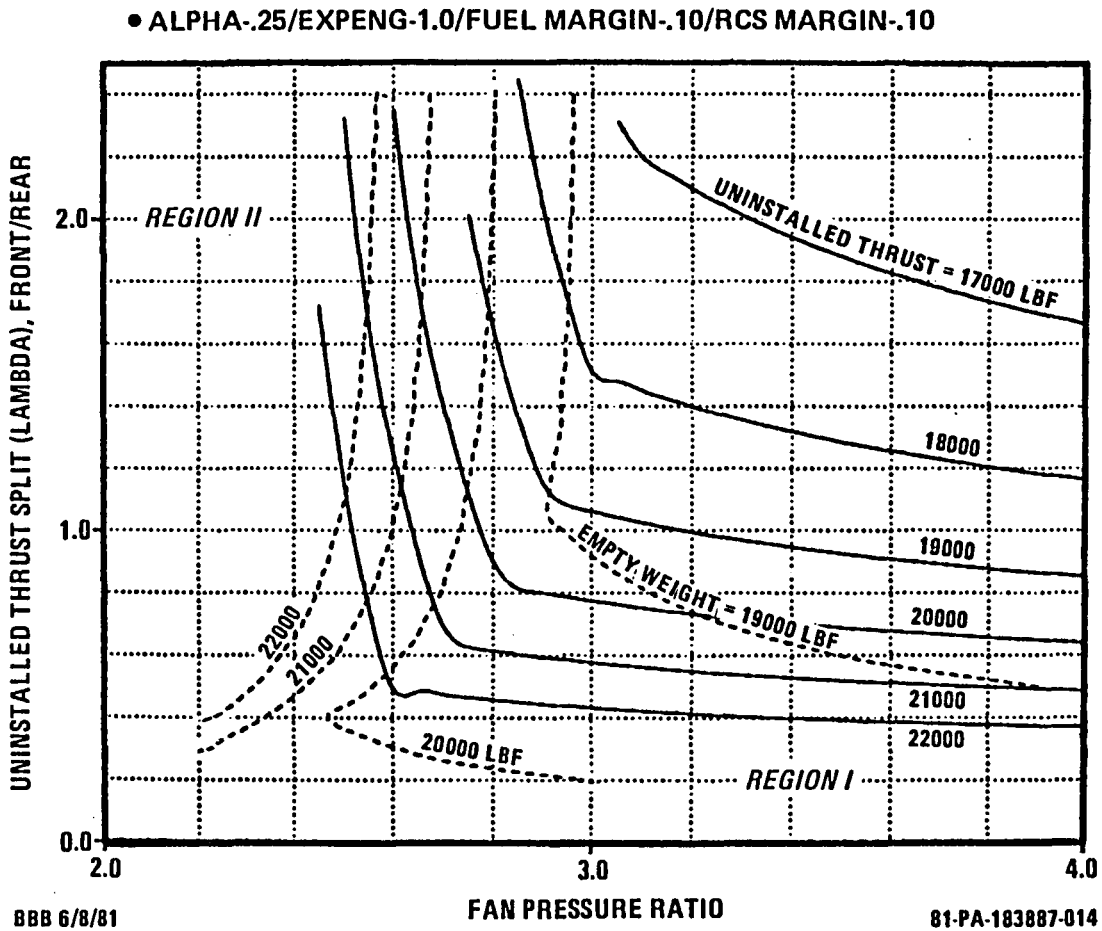

Figure 4-4 Minimum Uninstalled Engine Thrust Requirement (with Constant Empty Weight Lines)

area assumption. Weight growth is due primarily to growth in ejector size as FPR drops, engine and inlet size as thrust split drops, and the multiplier effect on engine weight. (a higher weight aircraft requires a higher thrust engine, which tends to be a higher weight engine, driving aircraft weight up again, etc.). Region II, on the left hand side of the plane, reflects configurations for which the core nozzle is located at the aft end of the ejectors, and for which wing growth is forced by changes in ejector size. Aircraft weight and required engine thrust are therefore very sensitive to changes in ejector size in this region.

Particular features of the constant parameter curves may be noted:

1.a. For a given empty weight, there is a minimum allowable fan pressure ratio, which occurs at the intersection of the constant weight line and the boundary between Regions I and II. Interpretation: Below this minimum FPR, ejector size increase forces the wing chord to increase, pushing up the empty weight. Hence there are no allowable fixed weight solutions for FPR's below this minimum. For higher FPR's in Region II, the higher thrust splits force ejector size up, driving wing size up. For higher FPR's in Region I, the lower thrust splits mean that the main engine thrust and weight must increase because of the reduced effect of thrust augmentation.

1.b. For a given fan pressure ratio, there is a minimum attainable empty weight, determined by the intersection of the constant fan pressure ratio line and the boundary between Regions I and II. Interpretation: This statement is the dual of statement 1.a.

2.a. For a given thrust split and empty weight, there is only one allowable fan pressure ratio. Interpretation: FPR's above (or below) the allowable FPR drive the aircraft weight strictly down (or up) at a fixed thrust split. Note the sensitivity of weight to fan pressure ratio in Region II.

2.b. For a given fan pressure ratio and empty weight, there are in general two allowable thrust splits. Interpretation: This statement is related to statements 1.a. and 1.b. above. The high thrust split solution lies in Region II and corresponds to large ejector size. The low thrust split solution lies in Region I and corresponds to large engine size. Note that some combinations of FPR and weight give degenerate or non-existent solutions.

In principle the λ-FPR map can be interpreted as defining a surface in a three-dimensional space whose coordinates are fan pressure ratio, uninstalled thrust split, and uninstalled thrust. The surface represents a level of minimum acceptable thrust. A particular engine can be represented by a point in that three dimensional space. Whether or not the engine is an acceptable candidate for the E-3 depends on whether the point falls above or below the minimum thrust surface. As discussed below, the thrust-weight methodology can be used to pick a design point for single variable parametric engines, for which the locus of possible engines is a curved line in three-dimensional space (one that hopefully intersects the minimum thrust surface). Thus, apart from being an interesting conceptual tool, the formalism can be applied to pick design points for most types of modifications engine manufacturers can make to provide engines for an E-X configuration.

As an example, for a time we contemplated using a refanned version of the Pratt and Whitney 1130 engine for the E-3. In order to pick a fan size, the engine manufacturer supplied data on uninstalled thrust split and thrust level, and engine weight as functions of

fan design flow rate. FPR was held constant. From this data, crossplots of λ vs. FPR, thrust vs. λ, and engine weight vs. thrust were made.

The weight vs. thrust data were input to the thrust-weight program, which generated a λ-FPR minimum uninstalled thrust map. The map was sliced along the given λ-FPR line to produce a plot of minimum acceptable thrust vs. λ. This line of minimum thrust was then superimposed on the engine line of thrust vs. λ, and the point of intersection of the two lines gave the minimum fan size for a feasible aircraft. This process is summarized in Figure 4-5.

The formalism is general enough to be applied to modifications other than refanning. As long as data for FPR, thrust split, engine thrust, and engine weight can be given in terms of a single parameter, the formalism can be applied to pick a design point for that parameter.

Although it was ultimately decided to stay with the groundrule that only existing engines with minor modifications be considered for E-X, the analysis of the interaction of thrust, thrust split, and fan pressure ratio enhanced our understanding of the requirements for and limitations on the propulsive system for E-X.

4.3 Applicability of the Various Engines

Based on the experience gained in laying out the various E-3 aircraft around the Rolls Royce 11F-35, the F101-GE-100, and the F101 DFE, and on the understanding derived from analysis of E-3 requirements, judgements could be made about the applicability of each of the candidate engines for the E-X. Table 4-1 gives a summary of the judgements made on the candidate engines.

The F101 DFE appeared to be the most viable engine candidate, because of doubts about the availability of the 11F-35 engine for the E-3 flight demonstrator. Further studies of the F101 DFE engine resulted in some optimizing of the nozzle control schedules of the engine to exploit the separated flow configuration, as discussed in the next section, which raised the thrust level sufficiently to make the F101 DFE a good candidate for the E-3 flight demonstrator. Subsequent studies of E-X focused on the E-X/F101 DFE configuration.

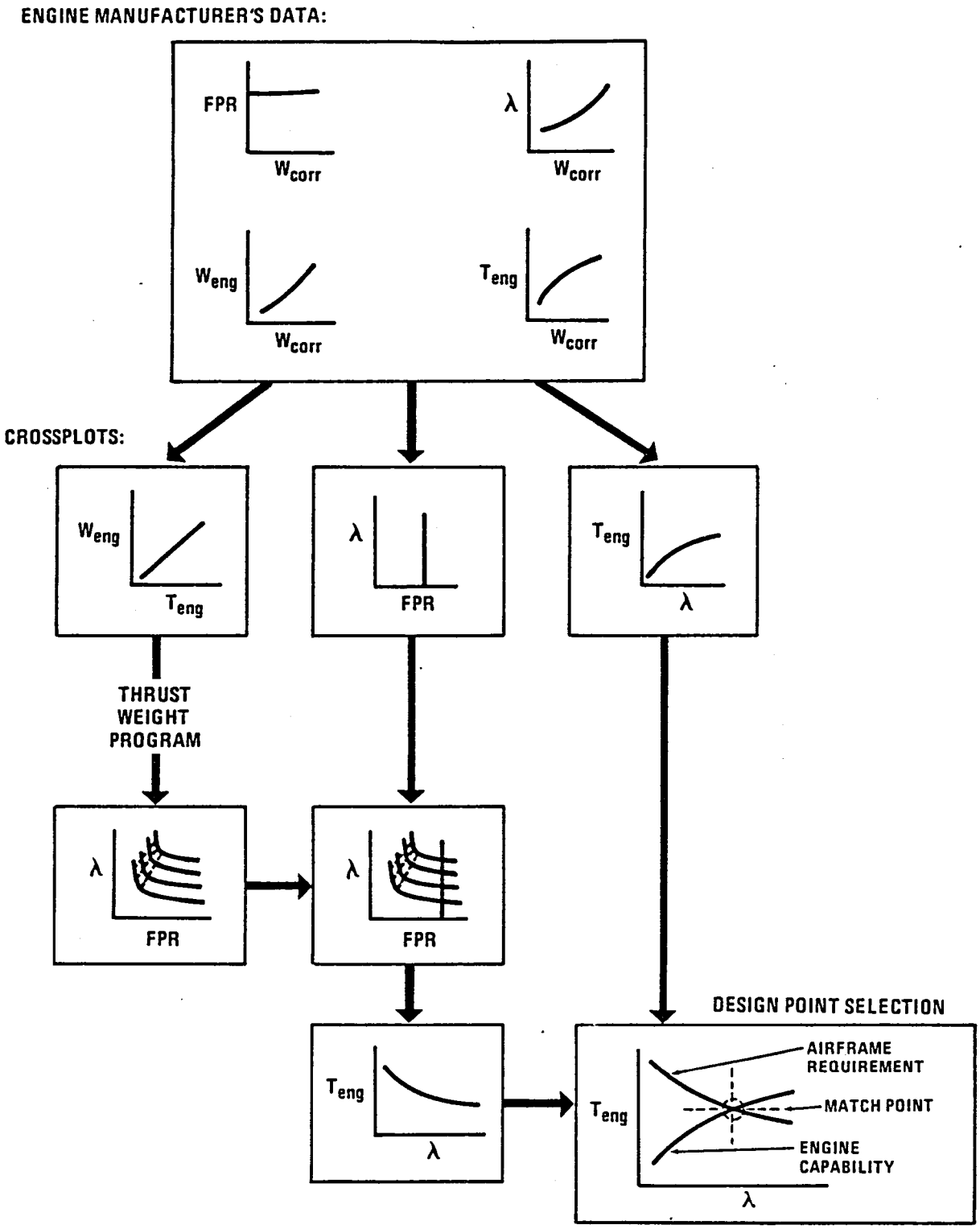

Figure 4-5 Thrust-Weight Formalism -Usage

ENGINE	COMMENT	ACCEPTABILITY
F101-GE-100	FPR TOO LOW – EJECTORS TOO LARGE	LOW
ENGINE 18	FPR MARGINAL – MAY NOT BE AVAILABLE FOR 1987 FLIGHT TEST	GOOD
ENGINE 4	FPR FAIR – MAY NOT BE AVAILABLE FOR 1987 FLIGHT TEST	FAIR
TF 41	FPR MARGINAL – THRUST LEVEL TOO LOW	LOW
ENGINE 16	THRUST LEVEL TOO LOW – POSSIBLE TWIN ENGINE CANDIDATE	REJECTED FOR SAFETY REASONS
F101 DFE	FPR GOOD – THRUST MARGINAL	FAIR
F101 DFE/A_J	FPR,THRUST SPLIT GOOD – THRUST LEVEL O.K.	GOOD

TABLE 4-1 ACCEPTABILITY OF CANDIDATE ENGINES

5. HOVER PERFORMANCE

A number of topics related to hover performance of the E-X/F101 DFE were treated analytically. The potential of the E-X/DFE for minimizing thrust loss due to reingestion when hovering was examined. An outgrowth of this study was an analysis of the variation of thrust split with ambient temperature, which emphasized the need for some system to compensate for static pitching moment variations induced by environmental or mechanical variables. As part of the effort to tailor the F101 DFE to the E-X configuration, the potential for exploiting the separation of the bypass and core was explored, providing partial solutions to optimizing thrust level and providing pitch control. A number of Reaction Control System concepts were examined, and a tentative candidate for the RCS was chosen. The effect of the gyroscopic moment of the engine on aircraft handling during hover was considered, and control system requirements were evaluated.

5.1 Reingestion

A major advantage of using ejectors to provide thrust augmentation is the potential for minimizing the loss of thrust that is due to reingestion of exhaust gases at the engine inlet. Ejectors, in marked contrast to various burner systems, produce exhaust air that is at a lower temperature than the primary air. Calculations based on the DeHavilland/Ames ejector test data indicate that the ejector primary air is diluted approximately 10 to 1 with ambient air.

Based on this data and on calculations of the sensitivity of the F101 DFE installed thrust and fan exit temperature, it is estimated that the loss in thrust due to reingestion for the DFE is approximately 1% for every 10% of inlet air that comes from the ejector exit. Although no satisfactory methodology exists for predicting the ejector exit to engine inlet reingestion fraction, figures on the order of twenty to thirty percent should be anticipated. This would imply a two to three percent loss of thrust, which is not unreasonable.

Another problem besides thrust loss that is related to hot gas reingestion is the reduction of fan stall margin due to total temperature distortion at the fan face. Any estimate of distortion due to reingestion is dependent on an estimate of reingestion fraction, but it is naturally expected that the distortion problem will be minimized with the lowering of exhaust gas temperature and velocity.

Graphs depicting thrust lapse due to reingestion and sensitivity to reingestion fraction for the F101 DFE installed in E-X are given in the proprietary volume of this report.

5.2 Thrust Split Variation with Ambient Temperature

During the study of the reingestion problem, it was noted that the core thrust and the bypass thrust varied with ambient temperature at different rates. This is essentially a result of the fan and core spool speed scheduling in the DFE, although other engines might be expected to display this phenomenon to some extent.

The significance of the variation of thrust split is that environmental (or mechanical) variables may affect the location of the propulsive center of thrust. Given the fixed axial location of the ejector and core nozzles, some method of compensating for the induced pitching moment caused by a mismatch of center of gravity and center of thrust must be incorporated in the design of E-X.

It would be worthwhile in a future stage of this program to identify all the variables, including variation in ejector performance, that could conceivably cause a shift in center of thrust, and then examine the worst case potential c.g. - c.t. mismatch in order to evaluate the capacity of any pitching moment compensation system for E-X.

A graph depicting the variation of core thrust and bypass thrust with ambient temperature is provided in the proprietary volume of this report.

5.3 A_J Control for the DFE Engine

The F101 DFE engine normally operates as a mixed flow engine. In the E-X configuration, however, the bypass and core flows remain unmixed. The unmixing of flows relieves the pressure matching constraint at the turbine exit and provides an additional degree of freedom in operating the engine.

This additional degree of freedom can be exploited to optimize the engine cycle for the proposed application. Subject to the other engine control system constraints, increasing the core jet area induces the following cycle adjustments in the engine:

a. The core NPR drops,
b. Low turbine power extraction increases,
c. The low spool speeds up,
d. The FPR increases,
e. The fan flow rate increases,
f. The core flow rate and fuel flow rate increase,
g. Fan thrust increases, and
h. Core thrust drops.

The increase in installed thrust is enhanced by the augmentation of the fan thrust as thrust is transferred from core to bypass flow.

Thus, the core A_J control can be used to increase the level of thrust over that which could be obtained by retaining the mixed flow cycle. At the E-X tropical day design point, this thrust increase amounts to about 5% over the mixed flow baseline, from 18117 lbf to 18939 lbf, due primarily to the shifting of flow to the augmented bypass stream.

In addition, the modulation of core jet area affects the fan to core thrust split. This effect can be exploited to provide at least partial pitch control at part power, if used in combination with another means of varying thrust and center of thrust simultaneously, as the power lever angle does, for example. It remains to be seen what further refinements can be made to this concept in order to tailor the F101 DFE to the E-X configuration.

5.4 Reaction Control System Concepts

For all V/STOL aircraft, some type of attitude control system is required in the hovering mode. In the past, this requirement has usually been met with a Reaction Control System (RCS) - a so-called "puffer-pipe" system which consists of high pressure gas ducted about the airframe and exhausted through nozzles at the wing tips, nose and tail.

The basic E-X concept is to use the RCS for both attitude control and vertical acceleration. The approach to the development of the particular RCS concept to be used in E-X was broad-based, and a number of concepts were examined. The general framework for the study specified RCS ports in the fore underbody, in the wing tips, and

in the aft underbody. Roll control is provided by the wing tip ports; pitch control by the forward port and the wing tip ports; and yaw control by the side-directed aft ports. (See Figure 5-1).

The pitch and roll ports only blow down in order to maximize vertical thrust.

A number of limitations and considerations are relevant to the choice of an RCS candidate. A stability and control analysis indicates that the system should have at least a 1000 lbf thrust capacity, directable to any of the ports. Duct size may be critical for some concepts, especially at the wing tips. Higher duct temperatures require insulation and generally heavier structures near the ducts. System weight and volume are important considerations, as is compatibility with aircraft lines. The RCS thrust itself should be controllable, be capable of modulation, and have a good response time. The system should be simple, stable, reliable, and maintainable. Other considerations arise during analysis; for instance, the potential for inlet reingestion of the forward pitch control port exhaust gases should be examined carefully for each concept.

5.4.1 RCS Candidates

Although the multiplicity of RCS candidates can be conceptually divided in several ways, it is most convenient to categorize them into airbreathing and non-airbreathing systems. The airbreathing category is taken to include engine powered systems as well as systems such as those using airbreathing auxiliary power units.

In general, the airbreathing systems are power-limited, that is, total thrust level is limited although continuous operation presents no major difficulties. On the other hand, non-airbreathing systems are energy-limited - they may be able to achieve much higher peak thrust levels than equivalent airbreathing systems, but total operating time is limited by the mass of propellant on board. The significant operating limitations for the two kinds of systems are therefore distinct, and equivalent but distinct duty cycles need to be defined for the two categories of RCS candidates.

For the purpose of quantifying the relative merits of the RCS candidates, airbreathing systems were sized to a 1000 lbf maximum thrust requirement. Based on a statistical analysis, this was found to be equivalent to approximately 300 lbf of time-averaged thrust for the purpose of calculating fuel consumption. Thus, non-airbreathing systems were sized for 300 lbf continuous thrust for a 10 minute duty cycle (a total of 180,000 lbf-sec of impulse), while retaining the requirement for a 1000 lbf maximum thrust capability.

Table 5-1 is an outline of the concepts examined in the RCS study. The list is not exhaustive, but rather reflects the broad basis of effort applied to this study.

5.4.2 Comparison of Candidates

Among airbreathing candidates, the principal competitors were direct main engine bleed and a load compressor system (a load compressor is simply an isolated air compressor driven by external shaft power input).

In terms of mechanical simplicity and operational reliability, main engine bleed is the most attractive system. No additional equipment besides ducting and regulators are required, and response time is very good. The ducting itself is compact due to the high pressure ratio available.

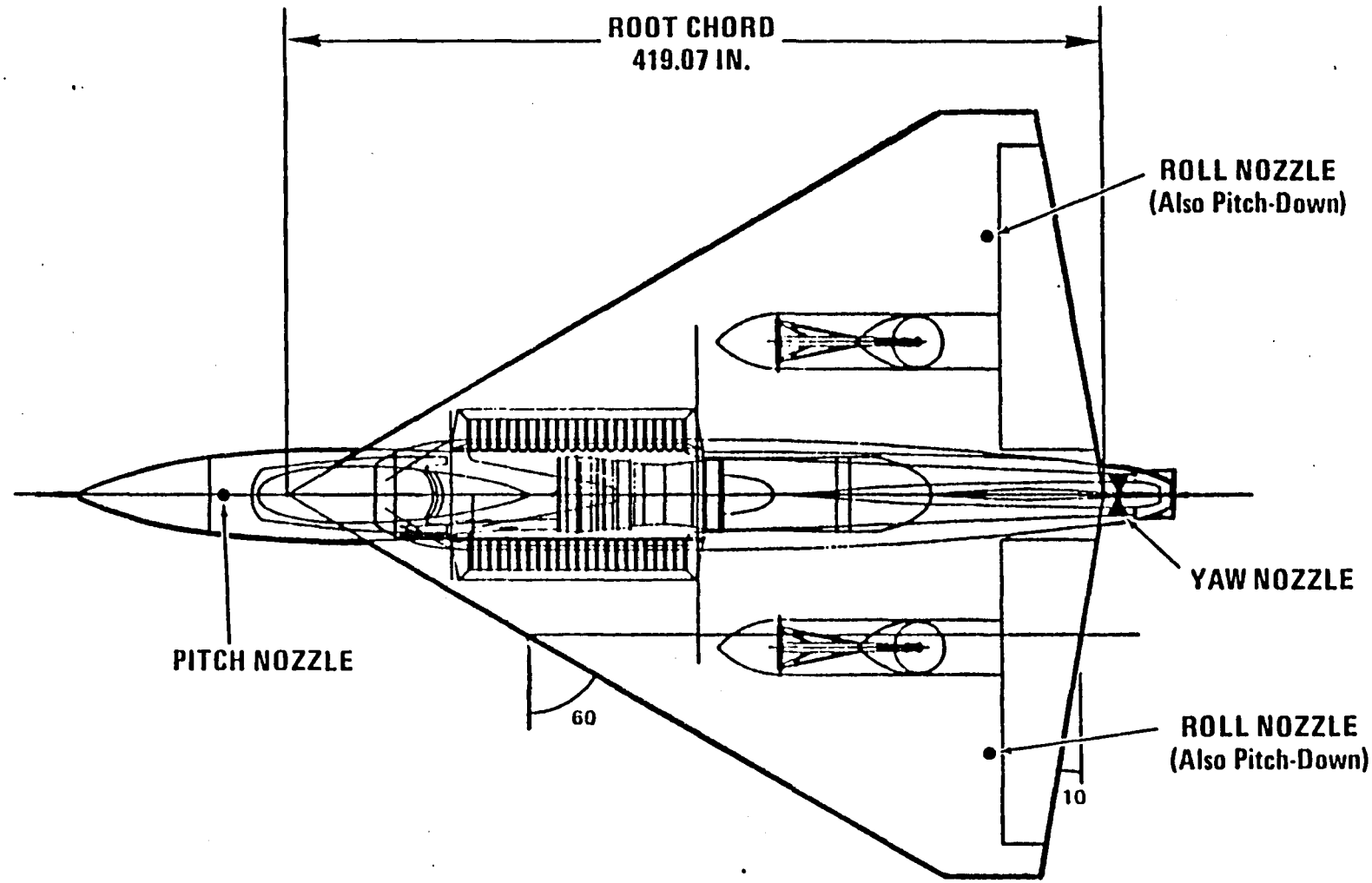

Figure 5-1 RCS Nozzle Locations

	COMMENTS
• AIRBREATHING SYSTEMS/ENGINE-POWERED SYSTEMS	Power Limited
• BLEED EXTRACTION	High Thrust Penalty
• LOAD COMPRESSOR	High Power Requirement
✔ Engine Powered	Exceeds Engine Capability
✔ APU Powered	Weight & Volume of APU Large
• LOAD COMPRESSOR-COMBUSTOR	Hot Ducting; Control Complexity
• STRAIGHT TURBOJET	FPR Too Low; Hot Ducting
• FLOW MULTIPLIERS	
✔ Ejectors, Tip Driven Fans, Etc.	NPR Too Low
• HYBRIDS	
✔ Bleed-Driven Flow Multipliers With Burning, Etc.	To be Investigated Case by Case
• NON-AIRBREATHING SYSTEMS	Propellant Weight (Energy) Limited
• HYDRAZINE	Dangerous
• LOX/JP-4	Propellant Weight
• PRESSURIZED/LIQUEFIED INERT GASES	Large Enthalpy Requirement

TABLE 5-1 RCS CONCEPTS

However, engine bleed degrades the thrust level of the engine and reduces the stall margin of the compressor. A graph depicting installed thrust vs. bleed extraction rate is given in the proprietary volume of this report. At the design point hover conditions, the DFE suffers a thrust loss of over 3000 lbf at the bleed extraction condition corresponding to 1000 lbf bleed thrust. This loss is unacceptable for a STOVL aircraft.

Although thrust lapse rates due to bleed were not investigated for all candidate engines, in general it is expected that the higher bypass ratio turbofans will be more sensitive to bleed fraction (bleed airflow/total engine airflow).

The next most attractive candidate is a load compressor system. Such a system has the advantage that the system design pressure ratio can be optimized, whereas a bleed system essentially operates at the main engine compressor discharge pressure. A load compressor system also has little or no effect on installed thrust, although system weight is larger than that of a bleed extraction RCS. The drawback to a load compressor system is the requirement for an external power source. For a given thrust level, nominally 1000 lbf, the power required to drive a load compressor is dependent on the system pressure ratio. Also, at a given thrust level, the nozzle exit area is a function of system pressure ratio. The desirable features of small duct areas and low power consumption are competing requirements in a load compressor system, the former requiring high pressure ratios and the latter, low. Figure 5-2 is a graph of power required versus nozzle throat area for load compressors designed to a 1000 lbf thrust requirement.

As can be seen, the power requirement is very large even for throat areas as large as 20 square inches. Duct and nozzle areas are critical for the RCS system, especially at the wingtips, where the available thickness for ducts tapers with spanwise distance. To some extent the problem can be alleviated with multiple parallel ducts, but increased duct losses then drive the system pressure ratio requirement up. Desirable nozzle throat areas are smaller than 10 square inches, for which power requirements exceed 2400 HP, and for which system operating pressure ratios exceed 7. To some extent this power requirement can be alleviated by utilizing one or more inline combustors in the ducting system, but only at the price of increased control complexity and hotter ducting.

Even with the inline combustor, the power requirement for a load compressor of the appropriate size exceeds the power extraction capability of the F101 DFE by a considerable margin. Among alternative power sources, a gas turbine used as an auxiliary power unit (APU) to drive the load compressor is the most obvious system to investigate further. Surveying the field of existing turboshaft engines, we noted that an Avco-Lycoming AL5512 engine is capable of supplying more than 4000 HP, requires a geometric envelope two feet in diameter and four feet long, and weighs approximately 700 lbf. The combination of the AL5512 and a properly sized load compressor appears to be a feasible RCS concept for the flight demonstrator.

A morphologically related concept is the use of a simple turbojet as a source of hot high-pressure air. However, given present-day turbine inlet temperatures and compressor pressure ratios, it appears that nozzle pressure ratios in the desired range (greater than 7) are unfeasible. Figure 5-3 shows the available nozzle pressure ratio for a turbojet with specified turbine inlet temperature and compressor pressure ratio.

A number of flow multiplier concepts were examined, including ejectors and tip-driven fans. However, because of the typically low nozzle pressure ratios that such devices employ, the units sized for 1000 lbf thrust tend to be bulky, reducing available fuel volume and creating compatibility problems with aircraft lines.

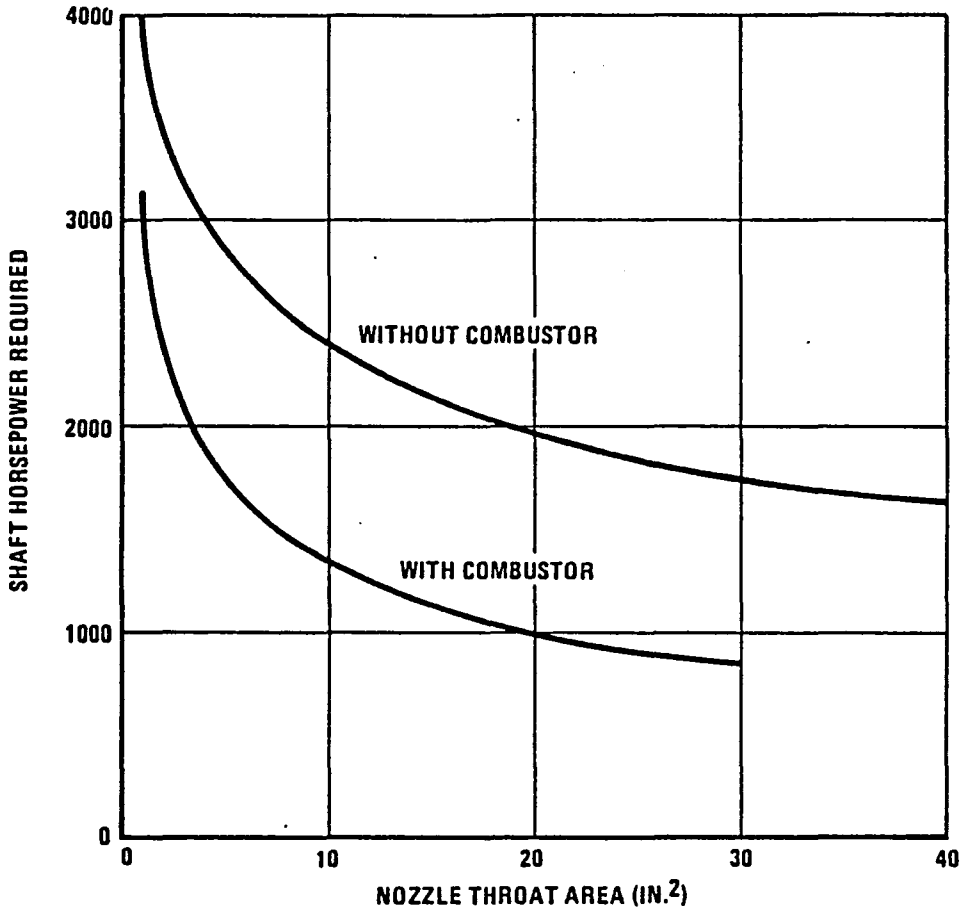

Figure 5-2 Shaft Horsepower versus Nozzle Throat Area for an RCS Load Compressor System

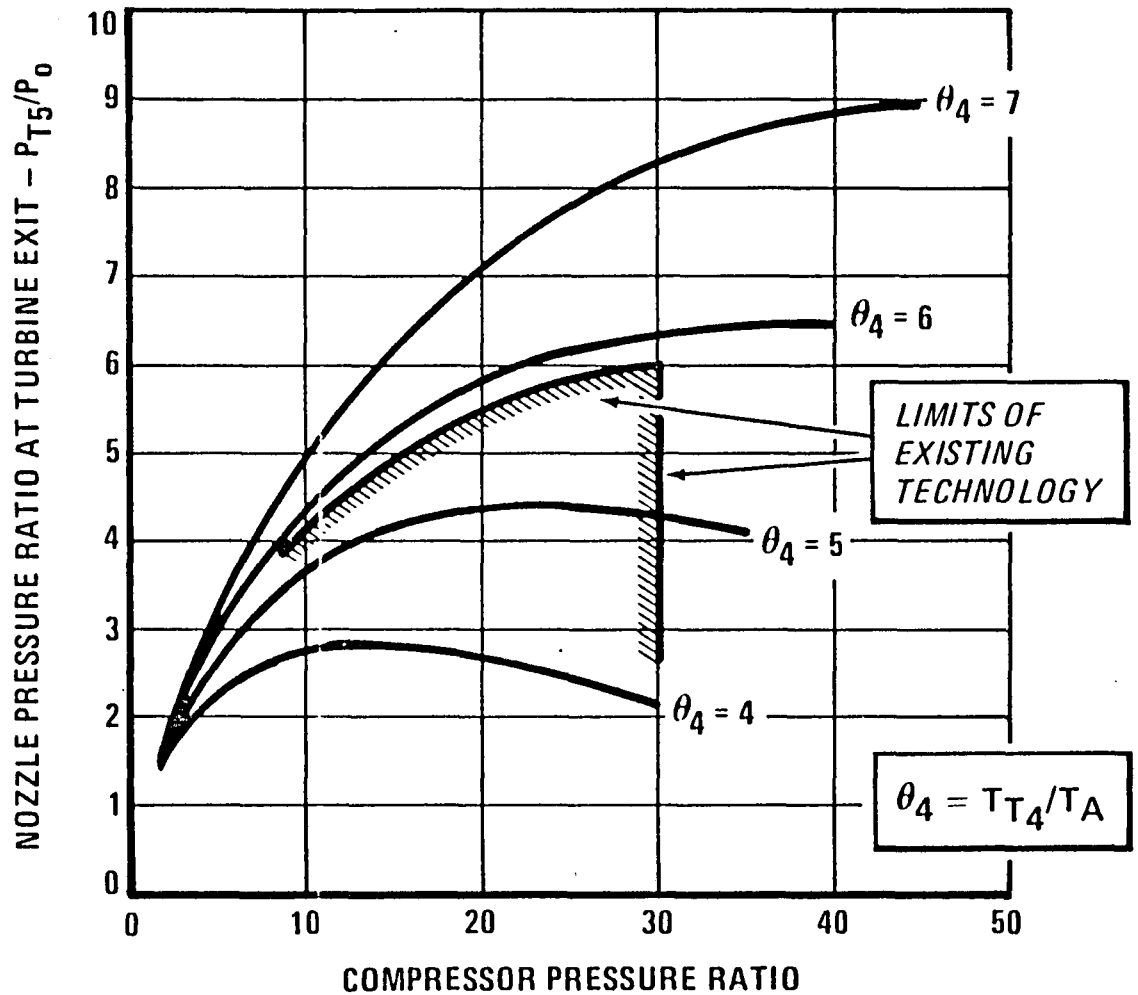

Figure 5-3 Simple Turbojet NPR versus CPR for Various Turbine Inlet Temperatures

A more promising flow multiplier concept takes engine bleed, expands it through a turbine, and uses the work to drive a compressor for ambient air. The expanded and compressed flows are brought to the same pressure and mixed together to form an exhaust stream. Garrett has conducted research into such mass flow multipliers, and we used some of their data in evaluating this concept.

Such a bleed-driven mass-flow multiplier is similar to a tip driven fan in concept, but the essential difference is that the exhaust pressure ratio at design point can be selected to be suitably high, i.e., around 7 or 8. The attractiveness of the system is predicated on the compressor discharge bleed of the main engine actually being of too high a pressure ratio (i.e., around 20) for efficient trades of thrust lapse and duct area. The prospect is that thrust loss in the main engine can be minimized by extracting a smaller amount of high pressure bleed and using the mass flow multiplier to augment the thrust while keeping duct areas and system size reasonable. Unfortunately, even with the addition of an inline combustor, it appears that the required bleed flow rates are still too high for an acceptable thrust loss. The concept merits further study, however, and it is possible that some innovation in configuration will reduce the bleed flow requirement. Future RCS studies should include this concept and its various hybrids.

Non-airbreathing systems have several potential advantages over airbreathing systems. In general, rockets will have a better response time than turbomachinery, providing better transient performance for the RCS. The ratio of peak thrust to design point thrust is also higher for rockets, allowing the system to operate closer to design point most of the time, while maintaining a peak thrust capability. If the propellant supply is centralized and distributed by a direct system, the ducts will be smaller than ducts for compressed gas with equivalent thrust capability.

However, the non-airbreathing candidates all suffer from the same drawback - the necessity of carrying the weight of oxidant on board the aircraft. Typical specific impulses are in the range of 250 to 300 seconds, and give total propellant masses in the range of 600 to 720 lb to achieve the target total impulse of 180,000 lbf-sec. This weight is exclusive of the weight of pressurized propellant containers, pumps, and control system apparatus. There is no weight advantage with rocket-type systems. This concern and the inherent problems with safety, operability, and reliability problems of these systems offset the advantages listed above. Thus, non-airbreathing systems appear less desirable than the APU/load compressor system outlined above.

5.5 Gyroscopic Effects

A critical contributor to the dynamic behavior of the aircraft in the hover mode is the angular momentum of the engine spools. The Rolls Royce Pegasus engines have counter-rotating low and high spools in order to minimize this gyroscopic effect, but the F101 DFE spools both rotate clockwise viewed from the rear. The total angular momentum of the spools will be

$$L = I_{low}\omega_{low} + I_{high}\omega_{high}$$

where I_{low} and I_{high} are spool inertias in lbm-ft^2 for the low pressure and high pressure spools, respectively,

and ω_{low} and ω_{high} are spool speeds in radians/sec.

The significance of this non-zero angular momentum can be seen by considering the response of the aircraft to various aerodynamic moments.

Rolling moments, either positive or negative, still tend to roll the aircraft. But pitching moments will tend to cause the aircraft to yaw, and yawing moments, to pitch, because of the precession of the angular momentum vector under an applied moment. For example, a positive yawing moment (clockwise viewed from the top) will cause the aircraft to pitch down; a negative yawing moment will cause the aircraft to pitch up. Figure 5-4 illustrates this effect.

Of course, the aircraft does not respond as a rigid rotating body of the same angular momentum would; the actual dynamic behavior of the aircraft/engine combination will be that of a massive static frame containing a gyroscope. This coupled dynamic behavior under applied torque is complicated, but can be characterized by the dimensionless ratio

$$\Psi = L^2_{engine}/(\tau_{applied} I_{aircraft})$$

where $\tau_{applied}$ = external torque applied, lbm ft^2/sec^2,
$I_{aircraft}$ = aircraft moment of inertia about axis of applied torque, lbm ft^2
L_{engine} = angular momentum of engine spools, lbm ft^2/sec

Ψ can be termed the gyro-static coupling parameter - for values of Ψ close to zero, the system behaves as an initially static body; for large values of Ψ, the system behaves as a pure gyroscope.

The value of Ψ for the E-7/F101 DFE in the sea level/static/tropical day mil power hovering mode can be calculated if an applied torque is specified. The yawing torque due to a gust at a given sideslip angle (i.e., the torque characterized by $C_{n\beta}$) is

$$\tau_{applied} = q\, Sc\, \beta\, C_{n\beta}$$

where q = dynamic pressure
S = reference wing area
c = reference mean chord
β = angle of sideslip

and $C_{n\beta}$ = derivative of yawing moment coefficient with respect to sideslip angle.

Values of S, c, and $C_{n\beta}$ can be found in Reference 5. For a 30 knot gust at a 30° sideslip angle and zero angle of attack, the torque is calculated to be

$$\tau_{applied} = 2100 \text{ lbf-ft} = 67{,}750 \text{ lbm } ft^2/sec^2$$

The aircraft inertia about the vertical axis can also be found in Reference 5.

$$I_{aircraft} = 65{,}788 \text{ slug-}ft^2 = 2.12 \times 10^6 \text{ lbm-}ft^2$$

The engine spool total angular momentum at tropical day military power is calculated to be

$$L_{engine} = 6.0 \times 10^5 \text{ lbm } ft^2/sec$$

Thus, the gyro-static coupling parameter for these conditions is

$$\Psi = L^2/(\tau I)$$
$$= 2.51$$

This near-unity value of Ψ shows that the aircraft dynamic behavior under these conditions, albeit dominated by gyroscopic effects, is significantly affected by the inertia of the static airframe.

Since the use of counter-rotating spools can reduce L_{engine} by an order of magnitude or more, depending on the relative speeds and inertias of the spools, and since the parameter Ψ is proportional to the square of L, the coupling parameter can be made quite small with such a system.

The gyroscopic effect should not increase the RCS requirements, since it does not alter the external torque applied to the airframe. However, it does alter the dynamic behavior of the aircraft and aircraft response to RCS thrust moments, and must be taken into account in designing the flight control system.

The E-X flight control system will monitor the spool speeds of the engine and process hover control responses based on these and other inputs.

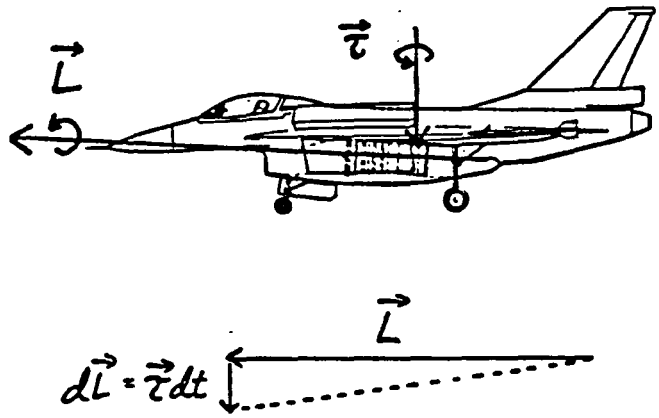

Positive Yawing Moment Causes Pitch-Down

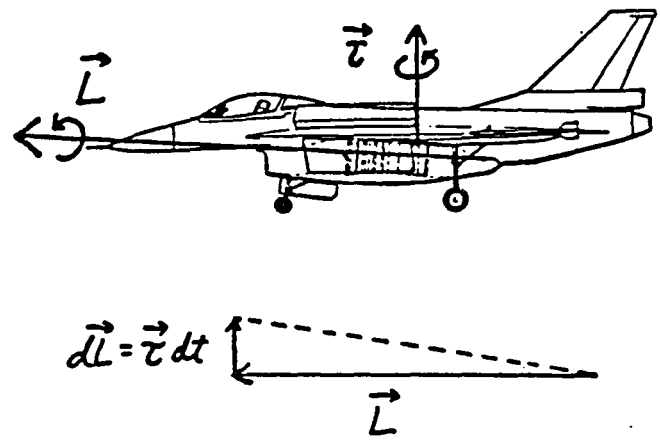

Negative Yawing Moment Causes Pitch-Up

Figure 5-4 Gyroscopic Effects

6. TRANSITION PERFORMANCE

The ejectors not only are used to provide thrust augmentation during vertical landing, but also are deployed during takeoff and transition to wingborne flight.

During transition, the bypass flow of the fan initially is directed entirely to the ejectors. As flight velocity increases, the flow is partially directed to the aft nozzle, further increasing vehicle acceleration. When fully wing-borne, all the bypass flow is directed to the aft nozzle. Modeling of this transfer of thrust from ejectors to aft nozzle was one outgrowth of our studies of transition performance.

Another area of concern was ejector ram drag. As flight velocity increases, the momentum drag of the ejector secondary airflow becomes a very significant component of total aircraft drag. The ram drag of the DHC/Ames ejectors was derived during the Ames tests, but it was unclear how the drag should be scaled for the ejectors in the E-X configuration. An analysis of ejector ram drag was carried out, and the results of that analysis were used to estimate the drag for the E-X configuration for transition studies.

6.1 Thrust Transfer

In order to model the transfer of thrust from the ejectors to the aft nozzle, the following assumptions were made:

1. The engine cycle was not modified during transfer (i.e., the bypass flow entrance conditions were fixed as functions of ambient conditions, altitude, and Mach number).

2. The ejector nozzles were assumed to have a fixed exit area and geometry.

3. The aft nozzle was assumed to have a fixed exit area and geometry.

4. The flow between the fan and the ejector nozzles, and between the fan and the aft nozzle, was assumed to be throttled to control the mass flow rate to the ejectors and aft nozzle, respectively.

Using these assumptions, the distribution of thrust during the transfer process can be characterized by the mass split fraction k, defined as

$$k = \dot{m}_{aft}/\dot{m}_{fan},$$

where $\dot{m}_{aft}$ = mass flow rate through aft nozzle

and $\dot{m}_{fan}$ = total bypass mass flow rate.

Then k = 0 when all the flow is sent to the ejectors and k = 1 when all the flow is sent out the aft nozzle (at the beginning and end of transition, respectively).

Once the mass flow, total temperature, and exit area are specified, the total pressure at the nozzle exit is determined (thus fixing the degree of throttling required), and the nozzle ideal thrust can be calculated. The tradeoff between ejector thrust and aft nozzle thrust is depicted in Figure 6-1 for a sample case of representative fan exit conditions. (A graph depicting ejector and aft nozzle thrusts for the E-X/F101 DFE configuration at varying Mach numbers is provided in the proprietary volume of this

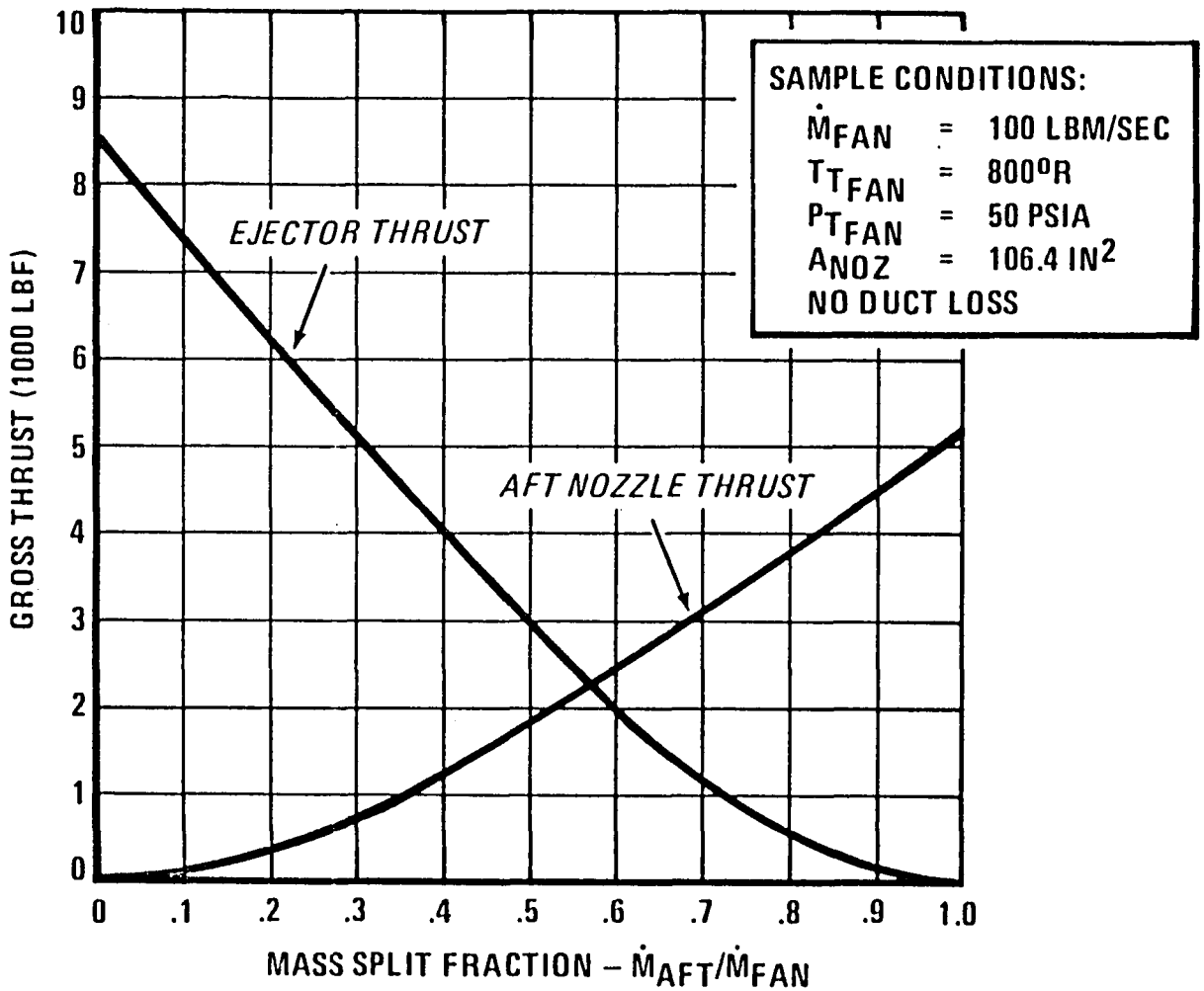

Figure 6-1 Ejector and Aft Nozzle Thrust as Functions of Mass Split Fraction -Fixed Area Aft Nozzle

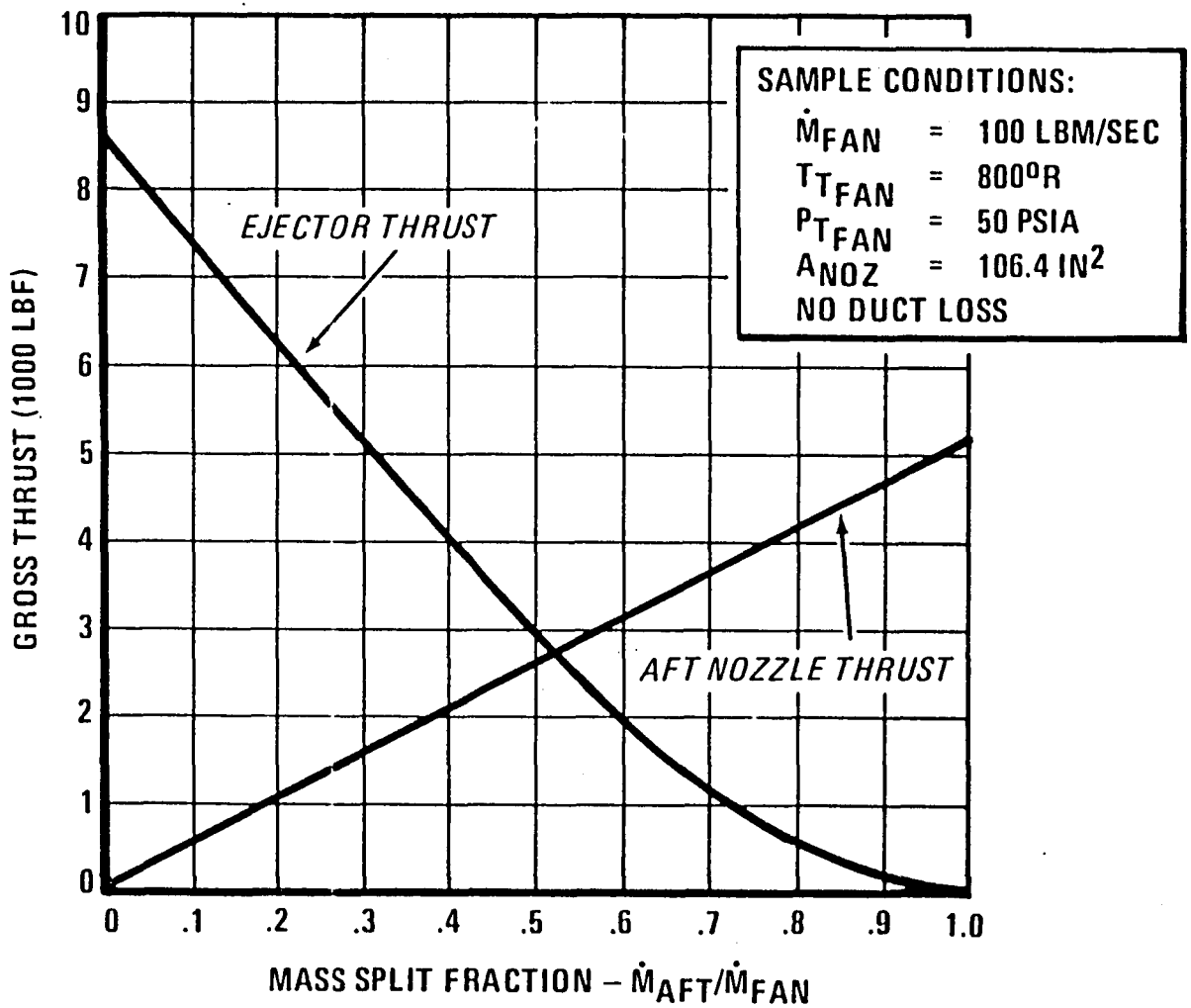

Figure 6-2 Ejector and Aft Nozzle Thrust as Functions of Mass Split Fraction -Variable Area Aft Nozzle

report). Figure 6-2 presents similar data for the case for which the aft nozzle flow is controlled by varying the nozzle throat area rather than by throttling. As can be seen, such a variable geometry system has thrust capability superior to a throttling system. However, the weight and complexity of a variable geometry nozzle is not generally justified on this basis alone, for the DFE or other engines; hence the non-afterburning flight demonstrator is assumed to utilize the dual throttle system, while the fully afterburning operational aircraft, which is equipped with a variable area aft nozzle, can exploit the advantage of variable area control over throttling control.

6.2 Ejector Ram Drag Analysis

Because the ram drag of the ejector secondary airflow is such an important component of the total aircraft drag, it was vital to accurate performance estimation to be able to model the ejector ram drag. In particular, a methodology was needed to apply the ram drag data derived from the Ames model test to the E-X ejectors, which are designed for a different flow size and pressure ratio. The goal of the ejector ram drag study was thus to derive a way of estimating the ram drag from known primary flow properties, system geometry, ambient atmospheric conditions, and dimensionless ejector performance parameters. Since the ram drag model was to be applied during transition, the primary flow parameters would have to reflect the throttling that was assumed in the thrust transfer modeling.

The ultimate result of this effort, details of which are to be found in Appendix A, is an equation which relates ejector ram drag to known or specified variables, allowing direct computation of the drag for various flight conditions. The analysis agrees well with and was calibrated using the Ames test data (Reference 2). This result was then used to predict ram drag for the various E-X configurations.

7. OPERATIONAL AIRCRAFT

The operational E-X aircraft will differ somewhat from the flight demonstrator. Most notably, it is envisioned that the operational aircraft will be fully afterburning in order to achieve the supersonic flight requirement. In modeling the performance of the E-X operational aircraft, a growth factor was applied to thrusts and fuel flows of the F101 DFE engine to approximate improvements in technology.

7.1 Afterburner Performance

Since the fan and core afterburners have not yet been designed, a simple model of burner performance, adequate for predesign purposes, was utilized. The model assumed a constant specific heat addition of enthalpy, with a 3600°R limit temperature and a 90% adiabatic fuel efficiency. Thrust augmentation was calculated based on the increase in temperature and mass flow. Because burner pressure loss is so dependent on flow Mach number and hence on geometry, and because the thrust is fairly insensitive to pressure loss at most of the up and away max power points, no additional pressure loss due to burning was assumed. However, an additional 4% pressure loss was assigned to the core flow due to the presence of afterburner equipment in the highly constrained core nozzle duct geometry. A total of 10% total pressure loss was taken in the bypass duct to account for ducting losses and the presence of afterburner equipment.

Our preliminary performance estimates indicate that both the fan and core afterburner are required for the aircraft to meet the type specification 169 criteria for maneuver and acceleration. Insufficient thrust is available with either the fan or core afterburner alone to meet either the turn load factor requirement at 0.65 Mach/10,000 ft or the acceleration requirement from .8 to 1.6 Mach at 35,000 Feet, but both criteria can be met with a dual augmentation system.

7.2 Growth Engine Requirements

Although the present F101 DFE engine, together with an AL5512 APU, will make an acceptable powerplant for an E-X flight demonstrator, the operational aircraft will require an engine with a higher thrust rating.

The range of growth engine requirements may be summarized by discussing two potential operational aircraft configurations: a threshold aircraft and a goal aircraft. The threshold aircraft is intended to represent a minimum acceptable configuration, while the goal aircraft represents a more desirable and capable configuration.

The threshold aircraft was specified as being able to hover with its operating weight empty, 5% of its takeoff fuel plus fuel for 4 minutes at intermediate power, plus two AIM-9's and two AMRAAM's. To meet these requirements, a 15% increase in tropical day mil power hovering mode thrust over the present DFE/A_J thrust level will be necessary. In addition, it is highly desirable to have the engine itself provide the reaction control system capability for the aircraft, so the threshold operational aircraft engine will have to supply high pressure bleed or horsepower extraction sufficient to provide 1200 lbf of RCS thrust, while sustaining the increased engine thrust level. The additional RCS requirement is due to the higher operating weight of the operational aircraft, compared to the flight demonstrator.

The goal operational aircraft has the same hovering requirements as the threshold aircraft, except that the allowance for landing with two AMRAAMs is uprated to an

allowance for 4000 lbs of payload beyond the fuel and AIM-9 allowance. This measure anticipates the deployment in the 1995 time-frame of expensive guided bombs which would be uneconomical to jettison if unused during a mission. The additional payload capability will require an increase of 32% in tropical day mil power hovering mode thrust over the present DFE/A_J thrust. In order to retain the same aircraft geometry as the E-X/F101 DFE, the goal engine will need a fan pressure ratio in the range of 4.0 to 4.5. The additional payload also pushes the RCS thrust requirement up to 1400 lbf.

In up and away flight, both the threshold and the goal aircraft have been assumed to have a modest 9% increase in thrust over the dual afterburning F101 DFE. Of course, the fan and core afterburners themselves will need to be developed for the operational aircraft. These growth engine requirements are summarized in Figure 7-1.

General Electric already has in place a near-term growth engine program to upgrade the thrust of the DFE by 9% in certain regions of the flight envelope. Since the operational E-X would be targeted for 1995 delivery, the threshold 15% growth in thrust over present day standards seems reasonable. The most difficult portion of the task may be getting the required RCS thrust while maintaining the target thrust level. As for the goal aircraft, it would appear that it would require a new engine altogether, since its thrust improvement is twice the threshold requirement and since the fan pressure ratio is considerably higher than that of the present day F101 DFE.

In order to get an estimate of reasonable engine growth rates, the thrust growth history of some U.S. gas turbine engines was researched. Figure 7-2 displays the percentage increase in thrust over a baseline thrust level as a function of elapsed time from a baseline year, for selected U.S. engines. The engines displayed are among the most successful gas turbines; many short-lived engines experience virtually no growth. However, the graph clearly shows that improvements of 10% to 20% over a 15-year time span are not unreasonable in a successful engine. It should be noted that none of the jumps in thrust level reflect the simple addition of an afterburner (such a drastic change would produce much larger thrust improvements). Two of the engines were designed as afterburning power plants (the J79 and the TF30), but two others had afterburners installed after the original design was established (the J85 and the J57); in the latter cases the baseline year and thrust were established for the afterburning version. The data in the chart are taken from Aviation Week's yearly specification summary.

Actual trades among growth engines of different manufacturers for the operational E-X aircraft were beyond the scope of this study, which was concerned with evaluating near-term engines for an E-X flight demonstrator aircraft.

✔FLIGHT DEMONSTRATOR:	PRESENT F101/DFE ENGINE (Baseline, T/W = 4.98*) + AL5512 APU (For RCS)	
✔THRESHOLD OPERATIONAL:	UP-AND-AWAY	9% THRUST INCREASE FOR POINT PERFORMANCE
	HOVER	15% THRUST INCREASE + H.P. BLEED OR POWER EXTRACTION SUFFICIENT TO PROVIDE 1200 LBS INSTALLED R.C.S. THRUST + FAN AIR A/B + T/W = 5.72*
✔GOAL OPERATIONAL:	UP-AND-AWAY	9% THRUST INCREASE FOR POINT PERFORMANCE
	HOVER	32% THRUST INCREASE WITH A FAN P.R. OF 4.5 + H.P. BLEED OR POWER EXTRACTION SUFFICIENT TO PROVIDE 1400 LBS INSTALLED R.C.S. THRUST + FAN A/B + T/W = 6.57*

**INT. POWER*

Figure 7-1 Powerplant Requirements for E-7

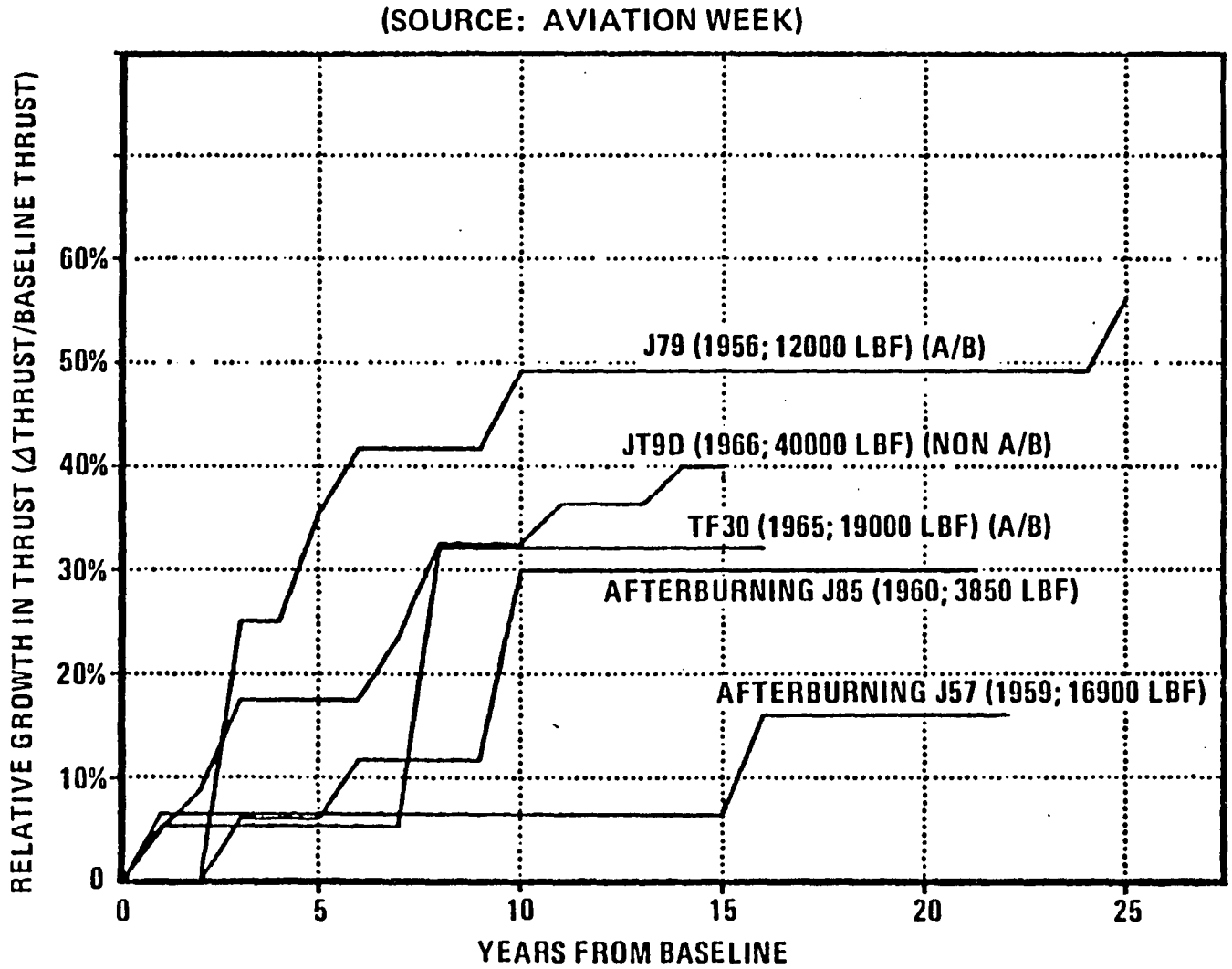

Figure 7-2 Thrust Growth History of Selected U.S. Gas Turbine Engines

8. SUMMARY

From the limitations on fan pressure ratio and thrust level imposed by the selection of the E-X configuration, the range of potential engines for E-X was narrowed to six candidates. Design point data were generated for each engine, and an E-3 type aircraft was laid out around two engines besides the original E-3 aircraft. Based on the experience gained from these layouts and on subsequent analysis, the General Electric F101 DFE engine was selected as the most suitable engine for an E-X flight demonstrator.

A number of topics dealing with the hovering mode and takeoff/transition mode were addressed. A Reaction Control System consisting of an Avco-Lycoming AL5512 turboshaft powering a load compressor was selected for the flight demonstrator. An analysis of ejector ram drag was carried out, allowing ram drag to be predicted from extrapolations of test data.

The capabilities of the present configuration DFE were compared with the requirements of an operational aircraft powerplant. A history of thrust growth for various engines was compiled, showing that reasonable growth of the DFE could make it an acceptable threshold engine for the operational E-X. However, the goal operational E-X will require a new engine.

9. RECOMMENDATIONS

Apart from the expected tasks of ejector development, inlet and nozzle design, and various model tests, further propulsion research is required to provide a sound basis for flight demonstrator aircraft design.

Future studies should address the task of matching the aircraft center of gravity with the propulsive center of thrust at the hover conditions. Environmental and mechanical variables which affect the thrust split of the engine should be identified, and worst case excursions from design point quantified, in order to support a rational estimation of pitch control system requirements.

The intermodulation of thrust level and thrust split with fuel flow and nozzle area control is a problem deserving of attention. The potential for cycle optimization at off-design conditions due to the addition of one more degree of operating freedom is worth exploring.

The Reaction Control System presently assumed for the flight demonstrator is not entirely satisfactory. Certain hybrids of the bleed flow multiplier concept may be more attractive candidates for the RCS, especially if coupled with improvements in engine thrust level. The potential for direct main engine bleed to power the RCS in the operational aircraft should also be evaluated realistically, in tandem with the other growth engine requirements.

This Page Intentionally Left Blank

APPENDIX A - EJECTOR RAM DRAG ANALYSIS

A.1 Introduction

During the transition from ejector-borne to wing-borne flight, the inlet momentum drag of the ejector secondary airflow is a significant contribution to total drag. It was therefore desirable to have an analytic method of predicting ejector secondary airflow and ram drag from measured ejector performance parameters, accounting for the changes in operating conditions in going from model data to full-scale performance. This analytic method was subsequently used in estimates of the transition characteristics of E-X aircraft.

This appendix documents in part the development of an ejector ram drag prediction methodology. The goal of this study was to estimate ejector ram drag from given primary flow properties, known system geometry, ambient atmospheric conditions, and dimensionless ejector performance parameters. The primary flow properties themselves reflected the throttling used to control the mass flow split between ejector and aft nozzle.

A.2 Control Volume

Figure A-1 depicts the control volume used in the ram drag study. The primary airflow is supplied from a reservoir at a total temperature $T_{Tsupply}$ and a total pressure $P_{Tsupply}$ in order to represent fan exit conditions. The flow is throttled to control the mass flow rate $\dot{m}_p$ through the primary nozzle area A_p. With an ideal throttle, primary air total temperature T_{Tp} will equal the supply total temperature, and primary air total pressure P_{Tp} will be a function of $\dot{m}_p$, T_{Tp}, and A_p. It is assumed that the primary airflow inlet momentum is accounted for elsewhere.

The secondary airflow is entrained at a rate $\dot{m}_s$ (to be solved for) and has the ram air total temperature T_{Ts}. It enters the control volume at the flight velocity V_∞, producing a momentum drag D in the negative axial direction.

The ejector exhaust has both an axial and a vertical component of velocity and hence of momentum flux. The subscript x refers to the axial direction, y to the vertical. The subscript e refers to exit plane conditions, which are assumed uniform. The exit area A_e is assumed to be known. A pressure matching condition at the ejector exhaust will be assumed.

Ambient conditions are denoted by T_a and P_a.

A.3. Basic Equations and Constitutive Relations

A.3.1 Momentum Relations

The ejector inlet momentum drag is given by

$$D = \frac{1}{g_c}\dot{m}_s V_\infty . \tag{1}$$

The recovered axial momentum thrust is

$$F_x = \frac{1}{g_c}\dot{m}_e V_x . \tag{2}$$

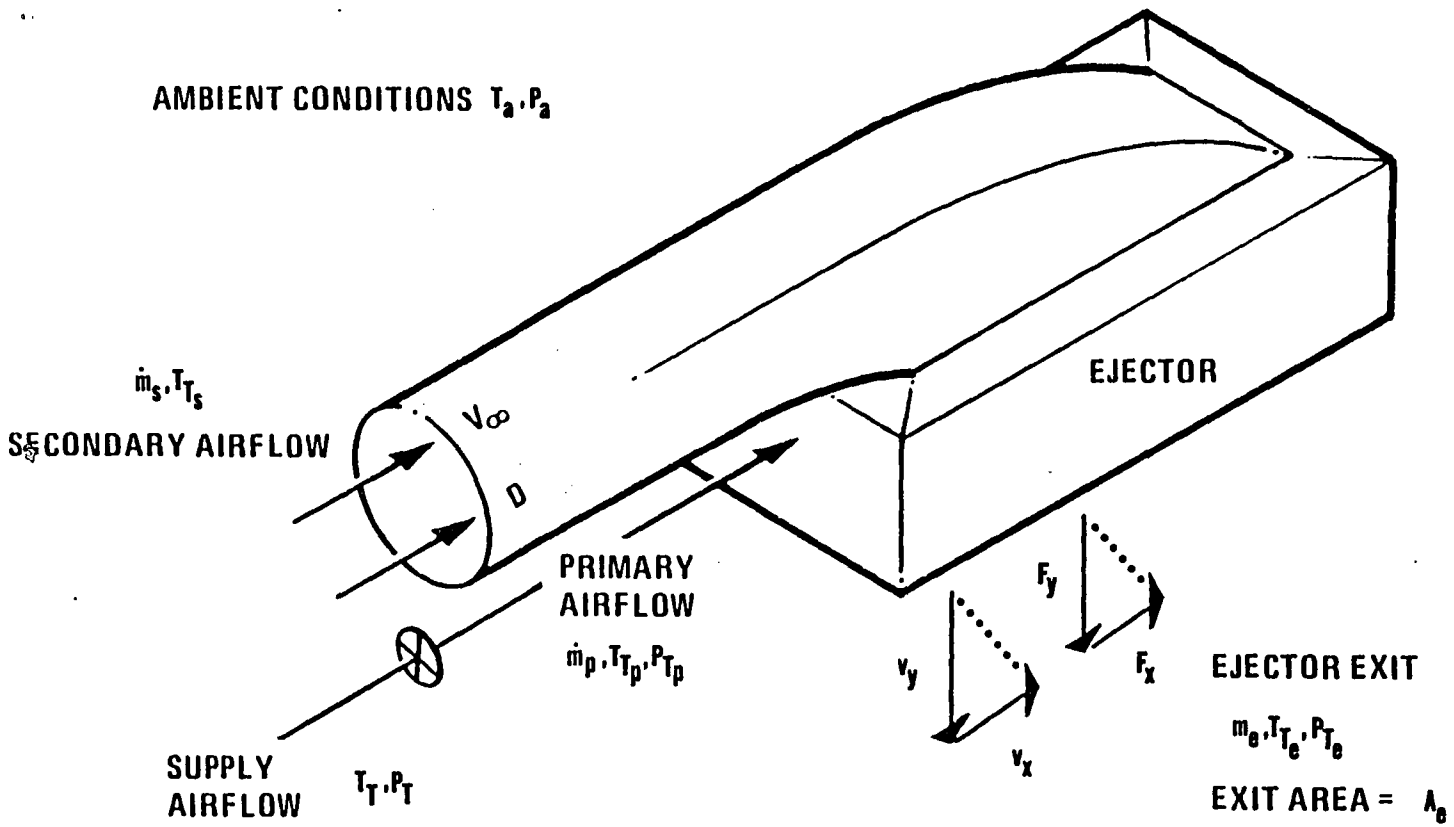

Figure A-1 Ejector Ram Drag Control Volume

We can then define an axial momentum recovery factor

$$\eta_a = \frac{F_x}{D} = \frac{\dot{m}_e v_x}{\dot{m}_s v_\infty}. \tag{3}$$

η_a is a dimensionless parameter describing ejector performance. In principle it is a function only of other dimensionless variables such as flight Mach number, primary to secondary temperature ratio, and geometric ratios. A knowledge of η_a can be derived from test data if drag and other relevant parameters are known.

The net axial drag force is thus

$$D - F_x = \frac{1}{g_c}(\dot{m}_s v_\infty - \dot{m}_e v_x) \tag{4}$$

$$= \frac{1}{g_c}(1 - \eta_a)\dot{m}_s v_\infty. \tag{5}$$

The ejector vertical thrust can be expressed as

$$F_y = \frac{1}{g_c}\dot{m}_e v_y. \tag{6}$$

F_y is related to the primary nozzle ideal thrust

$$F_{p_i} = \frac{\dot{m}_p}{g_c}\sqrt{\frac{2Rg_c\gamma}{\gamma - 1}T_{T_p}}\sqrt{1 - \left(\frac{P_{T_p}}{P_a}\right)^{\frac{1-\gamma}{\gamma}}} \tag{7}$$

by the ejector isentropic augmentation ratio

$$\phi = \frac{F_{G,\text{actual,vertical}}}{F_{G,\text{ideal,primary}}} = \frac{F_y}{F_{p_i}}. \tag{8}$$

ϕ is another dimensionless ejector performance parameter. A knowledge of ϕ will be required to predict net drag. Since primary nozzle flow conditions are assumed known, F_{p_i} and thence F_y will be known.

A.3.2 Continuity and Energy

The conservation of mass in a steady flow control volume implies

$$\dot{m}_e = \dot{m}_p + \dot{m}_s. \tag{9}$$

The ejector exit mass flow $\dot{m}_e$ can be written as

$$\dot{m}_e = \rho_{S_e} v_y A_e \tag{10}$$

where ρ_{S_e} is the static density of the gas at the ejector exit. By the ideal gas law,

$$\rho_{S_e} = \frac{P_{S_e}}{RT_{S_e}} \tag{11}$$

where P_{S_e} and T_{S_e} are the static pressure and temperature at the ejector exit.

A pressure matching at the ejector exit takes place. We will assume

$$P_{S_e} = P_a . \tag{12}$$

Mixing in the ejector is assumed to take place with constant enthalpy (no heat transfer or chemical reactions). Then

$$\dot{m}_e T_{T_e} = \dot{m}_s T_{T_s} + \dot{m}_p T_{T_p} . \tag{13}$$

The total temperatures can be expressed as

$$T_{T_e} = T_{S_e} + \frac{v_x^2 + v_y^2}{2c_p g_c} \tag{14}$$

and

$$T_{T_s} = T_a + \frac{v_\infty^2}{2c_p g_c} . \tag{15}$$

T_{Tp} is assumed to be known.

A.3.3 Ejector Primary Nozzle Pressure - Mass Flow Relation

In any nozzle, there exists a definite relation between mass flow rate, total temperature, exit effective area, and nozzle pressure ratio. Once we have specified the first three variables, the problem is to solve for the nozzle pressure ratio, in order that we may determine the thrust of the nozzle flow. The results may be summarized as

$$\frac{P_{T_p}}{P_a} = \begin{cases} \dfrac{\dot{m}_p \sqrt{T_{T_p}}}{D_1 P_a A_p} & \text{for } \dot{m}_p \geq \dot{m}_{ch,min} \\ \left(\dfrac{1}{2} + \dfrac{1}{2} \left(1 + 4 \left(\dfrac{\dot{m}_p^2 T_{T_p}}{\frac{2g_c}{R(\gamma-1)} P_a^2 A_p^2} \right) \right)^{\frac{1}{2}} \right)^{\frac{\gamma}{\gamma-1}} & \text{for } \dot{m}_p < \dot{m}_{ch,min} \end{cases} \tag{16}$$

where $\dot{m}_{ch,min} = D_1 P_a N_{ch,min} A_p \sqrt{T_{Tp}}$ = minimum choking mass flow

and $N_{ch,min} = \left(\frac{\gamma+1}{\gamma} \right)^{\frac{\gamma}{\gamma-1}}$ = minimum choking NPR

(Note $D_1 = .5317$ lbm R/lbf-sec = value of compressible flow function as Mach 1.0).

From this point the primary nozzle thrust can be calculated from Equation 7.

A.4 Solution of the System of Equations

The above system of equations are sufficient to solve for the secondary airflow and the ram drag of the ejectors. Heuristically, the derivation can be sketched as follows. Once the primary flow properties and augmentation ratio are specified, the ejector thrust is known. Thrust can be related to mass flow rate and velocity. The velocity is itself related to mass flow rate, area, and flow density. Density is a function of pressure and temperature. Flow temperature is related to mass flow rate because of the constant enthalpy mixing, and pressure is given by the pressure matching condition at the ejector exit. Thus, the mass flow rate can be related entirely to known parameters of pressure, area, and thrust, plus the primary flow properties. The momentum recovery is needed to determine the proportion of ram drag actually felt by the aircraft.

This derivation is outlined in Figure A-2.

The secondary mass flow rate $\dot{m}_S$ can be solved for as the root of the quadratic equation

$$(\dot{m}_s+\dot{m}_p)\left(\dot{m}_s+\dot{m}_p\frac{T_{T_p}}{T_{T_s}}\right)-\dot{m}_s^2\frac{\eta_a^2 V_\infty^2}{2c_p g_c T_{T_s}}=\frac{(g_c F_y)^2}{2c_p g_c T_{T_s}}\left(\frac{H+1}{H}\right) \tag{17}$$

where

$$H=\frac{1}{2}\frac{F_y}{P_a A_e}\frac{\gamma-1}{\gamma}. \tag{18}$$

This equation can be shown to have exactly one positive root for all reasonable values of system parameters.

A.5 Sample Calculations

Figures A-3 through A-6 present the results of some sample calculations for ejector net axial drag. The calculations assume sea level standard day ambient conditions, with primary airflow supply total temperature and total pressure of 800° R and 50 psia, respectively. The primary mass flow rate is expressed as a fraction of the supply flow rate of 100 lbm/sec. The flow is throttled to achieve the desired flow rate through the primary nozzles, which have a total effective area of 106.4 in^2. The ejector exit area is 32 times the primary nozzle area, or 3404.8 in^2.

For these calculations, the augmentation ratio ϕ was assigned a value of 1.60 and the momentum recovery η_a was assigned a value of 0.1.

Figure A-3 shows net axial drag $D-F_X$ vs. mass flow fraction k, for varying Mach number.

Figure A-4 shows ejector vertical thrust F_y vs. mass flow fraction k.

Figure A-5 is a crossplot of Figures 2 and 3, showing $D-F_X$ vs. F_y.

Figure A-5 shows a striking pattern: $D-F_X$ is apparently proportional to V_∞ and to $\sqrt{F_y}$. Hence, Figure A-6 presents $(D-F_X)/V_\infty\sqrt{F_y}$ vs. F_y. The dimensional group $(D-F_X)/V_\infty\sqrt{F_y}$, which shall henceforth be termed the ejector ram drag parameter and denoted by α_R, is fairly constant for the range of F_y and V_∞ shown in the figure. α_R is clearly useful for approximating performance.

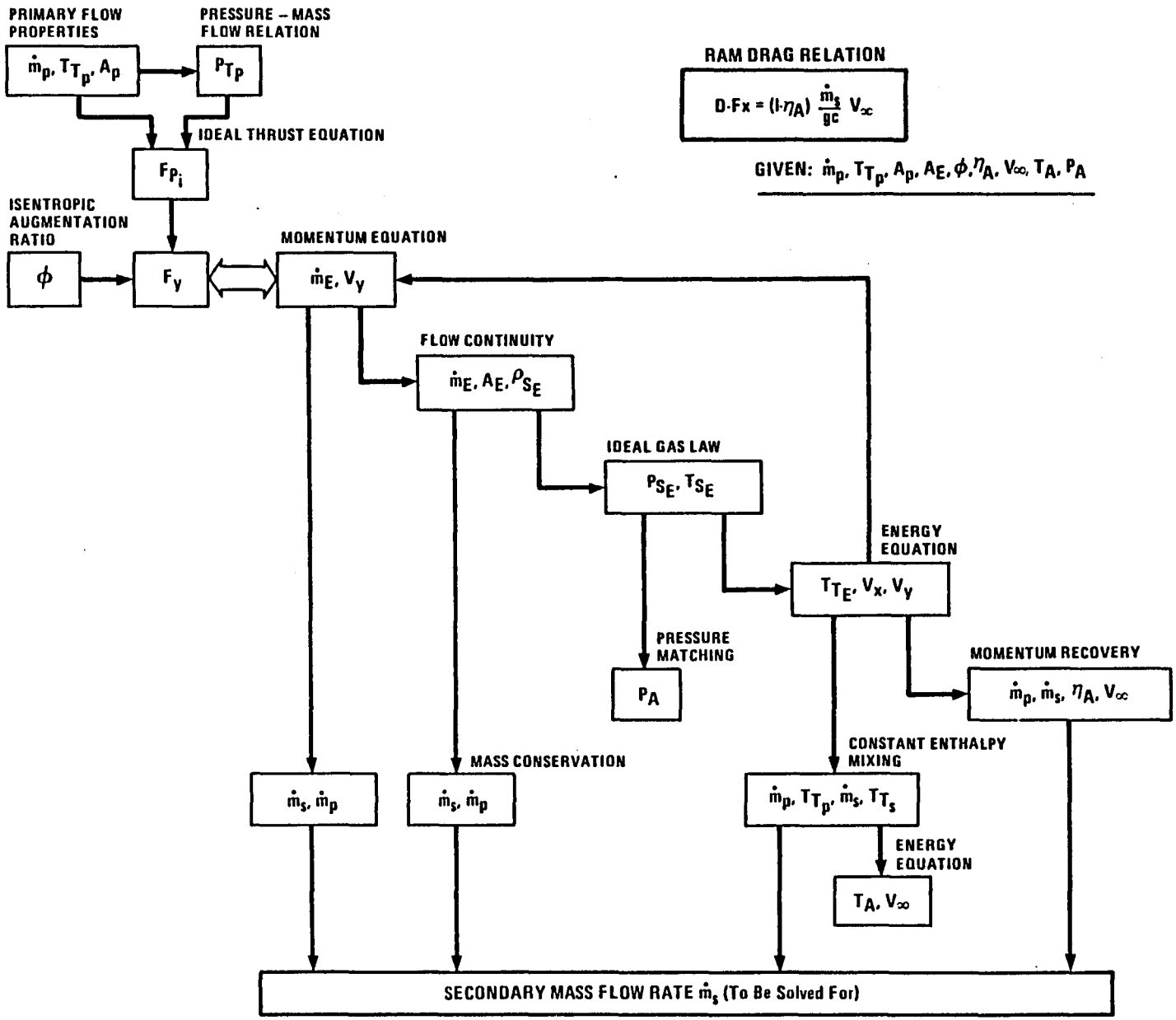

Figure A-2 Block Diagram for Deriving Mass Flow Rate Relation

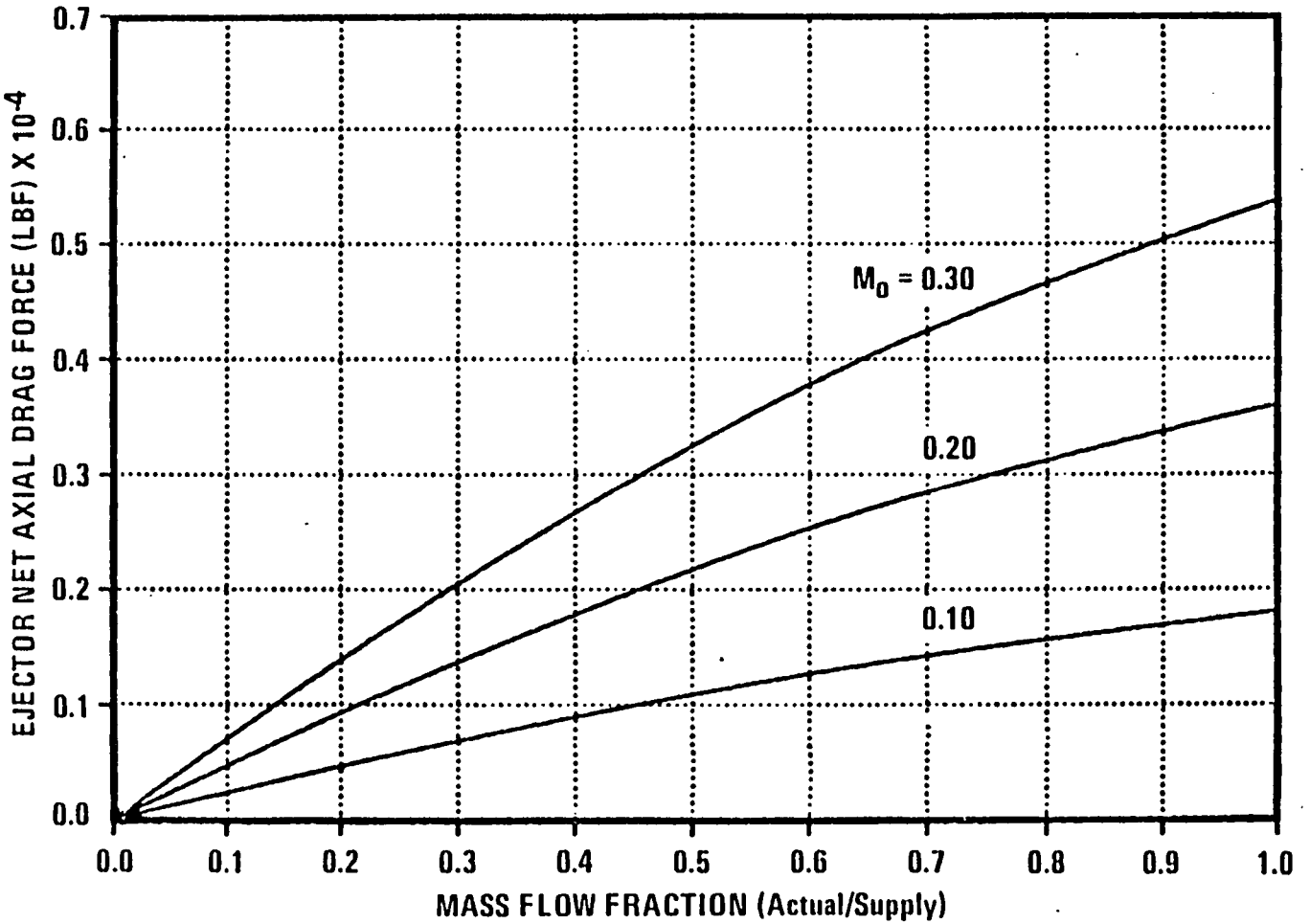

Figure A-3 Ejector Net Axial Drag vs. Mass Flow Fraction

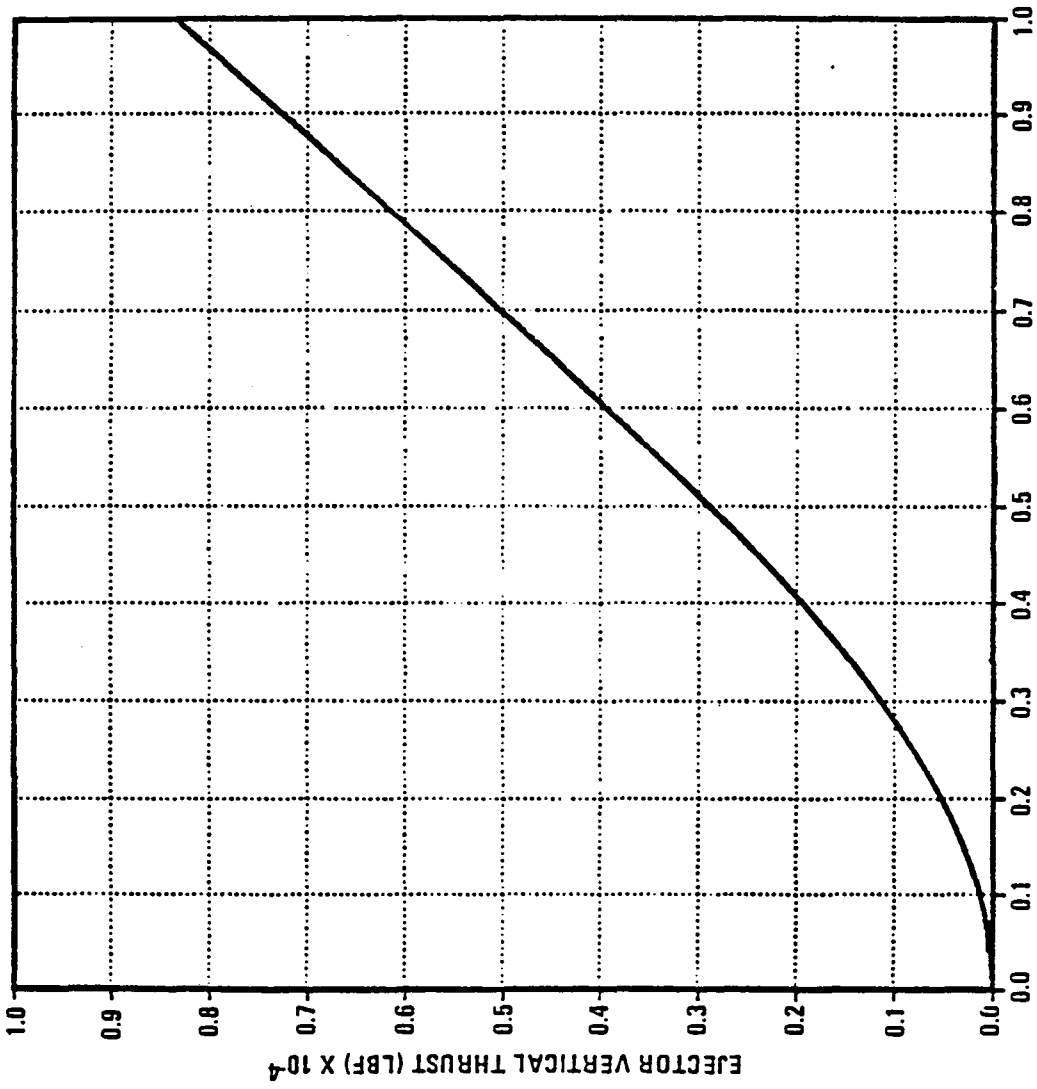

Figure A-4 Ejector Vertical Thrust vs. Mass Flow Fraction

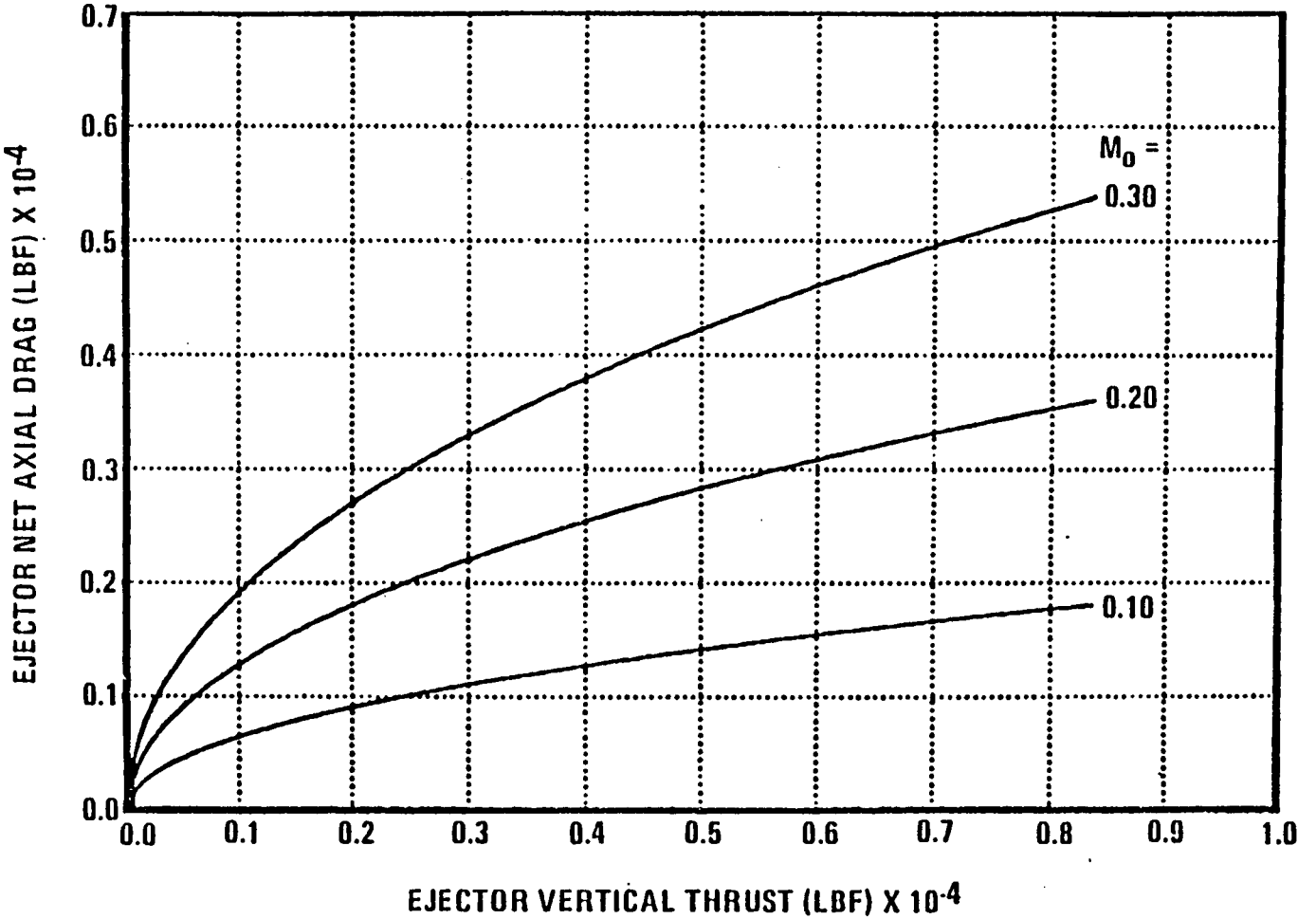

Figure A-5 Ejector Net Axial Drag vs. Ejector Vertical Thrust

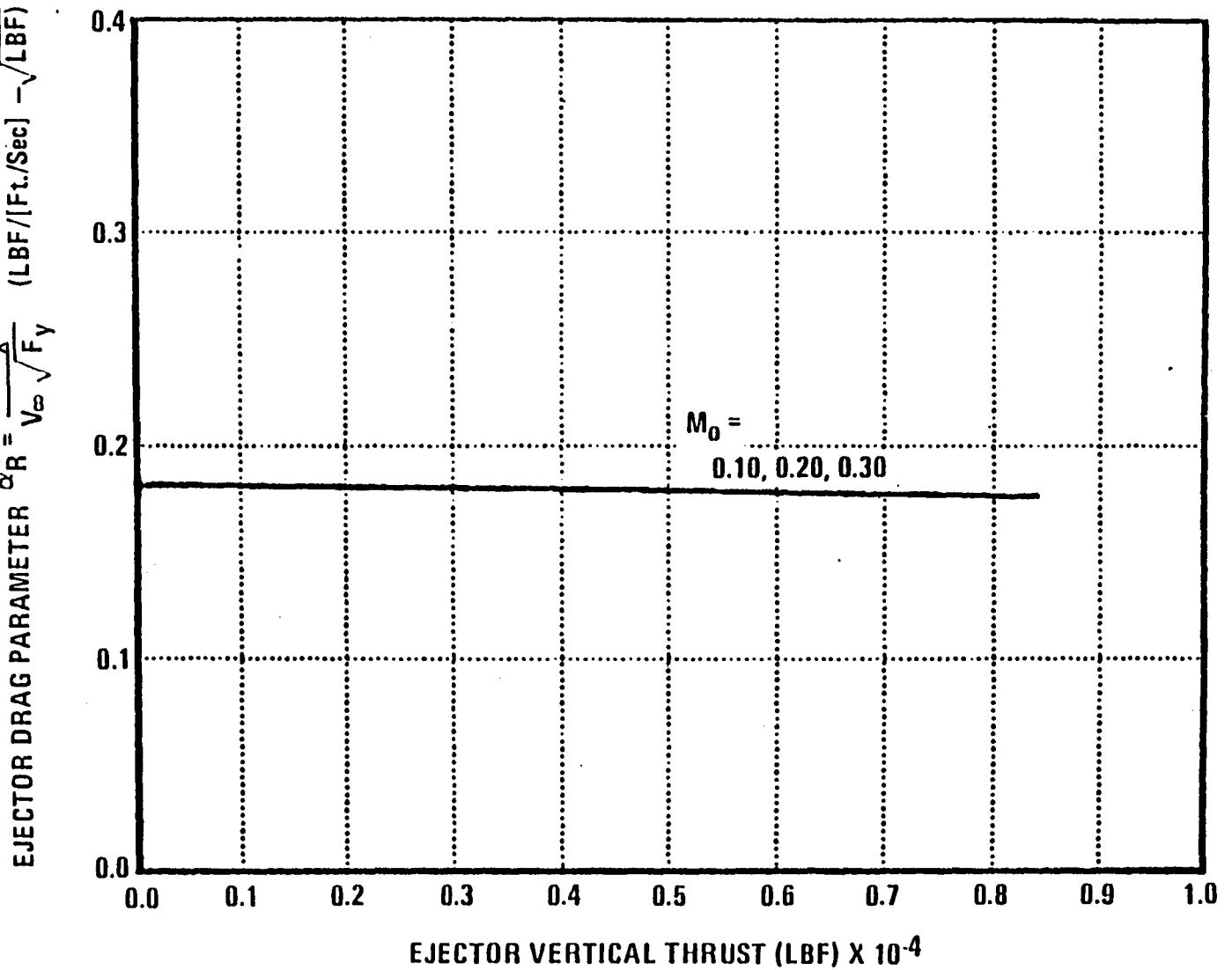

Figure A-6 Ejector Ram Drag Parameter vs. Ejector Vertical Thrust

A.5.1 Approximate Expression for α_R

Manipulation of the expression for $\dot{m}_s$ yields the following approximation for α_R.

$$\alpha_R \equiv \frac{D - F_x}{v_\infty \sqrt{F_y}} \cong (1 - \eta_a)\left(\sqrt{\frac{P_a A_e}{g_c R T_{T_s}}} - \sqrt{\frac{P_a A_p^{\frac{\gamma+1}{2}}}{g_c R T_{T_p}}} \left(\frac{\frac{T_{T_p}}{T_{T_s}}+1}{2}\right)\right). \tag{19}$$

Note that $$\alpha_R \cong \sqrt{A_e}. \tag{20}$$

Among other things, this result implies that a system operating at the same thrust level but a lower primary air pressure ratio will have a higher ram drag than a high pressure ratio system, because of the increased flow area.

A.6 Comparison With Test Data

Figure A-7 gives a comparison of the above analysis with empirical data from large scale ejector tests conducted at NASA Ames' 40x80 wind tunnel (Reference 2). The Ames tests were carried out with DeHavilland - type ejectors.

The figure shows both the net axial drag of the test ejectors, as interpreted by the Ames experimenters, and the predictions of net axial drag based on Equation 17, for several values of η_a. The following parameters were assumed in the calculation of theoretical drag.

P_{Tp}/P_a = 2.5,

T_{Tp} = 700° C = 1752° R,

A_p = 91.4 in^2,

A_e = 2924.8 in^2,

$\dot{m}_p$ = 42.66 lbm/sec (consistent with the above),

ϕ = 1.63,

T_a = 549.5° R (tropical day),

and P_a = 14.696 psia.

The graph shows good agreement between the measured and calculated values of axial drag for values of η_a for the DHC ejectors ranging between 0 and 0.1. A principal unknown is the effective value of ϕ for these wind-on measurements; this uncertainty could have a significant effect on the comparison.

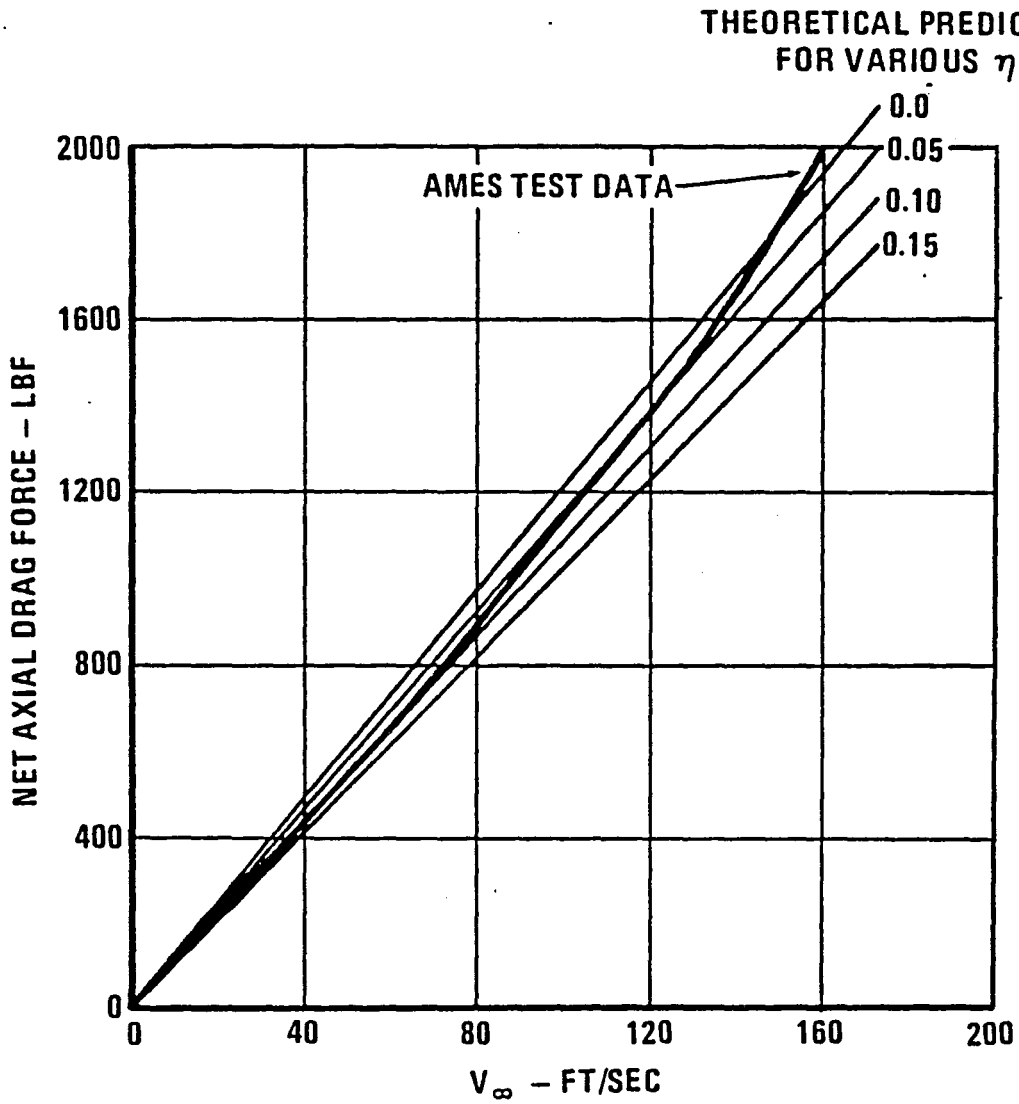

Figure A-7 Comparison of Ram Drag Theory with Test Data

A.7 Summary

Ejector secondary airflow can be calculated as the positive root of the quadratic equation

$$(\dot{m}_s+\dot{m}_p)(\dot{m}_s+\dot{m}_p\frac{T_{T_p}}{T_{T_s}}) - \dot{m}_s^2\frac{\eta_a^2 v_\infty^2}{2c_p g_c T_{T_s}} = \frac{(g_c F_y)^2}{2c_p g_c T_{T_s}}\left(\frac{H+1}{H}\right) \tag{7}$$

where $$H = \frac{1}{2}\frac{F_y}{P_a A_e}\frac{\gamma-1}{\gamma}.$$

Drag can then be calculated from

$$D - F_x = \frac{1}{g_c}(1-\eta_a)\dot{m}_s v_\infty. \tag{5}$$

The quantity $(D-F_x)/V_\infty\sqrt{F_y}$ is fairly constant for ranges of V_∞ and F_y. It is denoted by the α_R and can be approximated by

$$\alpha_R \equiv \frac{D-F_x}{v_\infty\sqrt{F_y}} \equiv (1-\eta_a)\left(\sqrt{\frac{P_a A_e}{g_c R T_{T_s}}} - \sqrt{\frac{P_a A_p}{g_c R T_{T_p}}^{\frac{\gamma+1}{2}}}\left(\frac{\frac{T_{T_p}}{T_{T_s}}+1}{2}\right)\right). \tag{19}$$

Drag is then proportional to $\sqrt{A_e}$ and is therefore greater for lower pressure ratio systems.

The agreement between theory and experiment is good.

A.8 Conclusions

The analysis presented in this Appendix provides a straightforward means of predicting ejector secondary air net axial drag, once certain ejector performance parameters are known, and primary air and ambient conditions have been specified.

For preliminary design purposes, the ejector ram drag parameter α_R can be approximated and assumed constant. An expression for α_R is given above.

Agreement between theory and experiment is good.

This Page Intentionally Left Blank

APPENDIX B. UNIT CONVERSIONS

U.S. Customary Units have been used for dimensional quantities throughout the report text. This appendix provides conversion factors to the International System (SI) of units taken from Reference 7.

To Convert From	To	Multiply By
ACCELERATION		
foot/second^2	meter/second^2	3.048 E-01
AREA		
foot^2	meter^2	9.290 304 E-02
inch^2	meter^2	6.4516 E-04
DENSITY		
lbm/inch^3	kilogram/meter^3	2.767 990 5 E+04
lbm/foot^3	kilogram/meter^3	1.601 846 3 E+01
slug/foot^3	kilogram/meter^3	5.153 79 E+02
ENERGY		
British thermal unit	joule	1.055 056 E+03
foot lbf	joule	1.355 817 9

To Convert From	To	Multiply By
FORCE		
lbf (pound force, avoirdupois)	newton	4.448 221 615 260 5
LENGTH		
foot	meter	3.048 E-01
inch	meter	2.54 E-02
nautical mile (U.S.)	meter	1.852 E+03
statute mile (U.S.)	meter	1.609 344 E+03
MASS		
pound mass, lbm (avoirdupois)	kilogram	4.535 923 7 E-01
slug	kilogram	1.459 390 29 E+01
POWER		
foot lbf/second	watt	1.355 817 9
horsepower (550 foot lbf/second)	watt	7.456 998 7 E+02
PRESSURE		
atmosphere	newton/meter^2	1.013 25 E+05
inch of mercury (32^{o}F)	newton/meter^2	3.386 389 E+03
inch of mercury (60^{o}F)	newton/meter^2	3.376 85 E+03
inch of water (39.2^{o}F)	newton/meter^2	2.490 82 E+02

To Convert From	To	Multiply By
inch of water (60°F)	newton/meter^2	2.4884 E+02
lbf/foot^2	newton/meter^2	4.788 025 8 E+01
lbf/inch^2 (psi)	newton/meter^2	6.894 757 2 E+03
millibar	newton/meter^2	1.00 E+02
millimeter of mercury (0°C)	newton/meter^2	1.333 224 E+02
torr (0°C)	newton/meter^2	1.333 22 E+02
SPEED		
foot/second	meter/second	3.048 E-02
kilometer/hour	meter/second	2.777 777 8 E-01
knot (international)	meter/second	5.144 444 444 E-01
mile/hour (U.S. statute)	meter/second	4.4704 E-01
TEMPERATURE		
Celsius (t_C)	Kelvin (t_K)	$t_K=t_C+273.15$
Fahrenheit (t_F)	Kelvin	$t_K=(5/9)(t_F+459.67)$
Fahrenheit	Celsius	$t_C=(5/9)(t_F-32)$
Rankine (t_R)	Kelvin	$t_K=(5/9)t_R$
VISCOSITY		
foot^2/second	meter^2/second	9.290 304 E-02
lbm/foot second	newton second/meter^2	1.488 163 9
lbf second/foot^2	newton second/meter^2	4.788 025 8 E+01
slug/foot second	newton second/meter^2	4.788 025 8 E+01

To Convert From	To	Multiply By
VOLUME		
foot^3	meter^3	2.831 684 659 2 E-02
gallon (U.S. liquid)	meter^3	3.785 411 784 E-03
inch^3	meter^3	1.638 706 4 E-05

REFERENCES

1. D.B. Garland, Static Tests of the J-97 Powered, External Augmentor V/STOL Wind Tunnel Model, DeHavilland Report DHC-DND 77-4, February 1978.

2. D.B. Garland, Phase 1 Wind Tunnel Tests of the J-97 Powered, External Augmentor V/STOL Model, DeHavilland Report DHC-DND 79-4, September 1979.

3. D.B. Garland and J.L. Harris, Phase 2 and 3 Wind Tunnel Tests of the J-97 Powered, External Augmentor V/STOL Model, DeHavilland Report DHC-DND 80-1, March 1980.

4. F.L. Gilbertson, and D.B. Garland, Static Tests of the J-97 Powered, External Augmentor V/STOL Model at the Ames Research Center, DeHavilland Report DHC-DND 80-2, 1980.

5. W. H. Foley et al, Study of Aerodynamic Technology for Single-Cruise-Engine V/STOL Fighter Attack Aircraft, NASA CR 166268, February 1982.

6. D.C. Whittley and D.G. Koenig, Large Scale Model Tests of a New Technology V/STOL Concept, AIA 80-0233, AIAA 18th Aerospace Sciences Meeting (January 14-16, 1980) Pasadena, California.

7. Mechtly, E. A., The International System of Units: Physical Constants and Conversion Factors, NASA SP-7012, 1973.

1. Report No.	2. Government Accession No.	3. Recipient's Catalog No.
NASA CR-166304		

4. Title and Subtitle	5. Report Date
An Engine Trade Study For a Supersonic STOVL Fighter/Attack Aircraft (Volume I)	February 1982
	6. Performing Organization Code: -

7. Author(s)	8. Performing Organization Report No.
B. B. Beard and W. H. Foley	-

9. Performing Organization Name and Address	10. Work Unit No.
General Dynamics Fort Worth Division P.O. Box 748 Fort Worth, Texas 76101	T-5517
	11. Contract or Grant No.: NAS2-10981
	13. Type of Report and Period Covered: Contractor Final Report June 1981 to February 1982
12. Sponsoring Agency Name and Address National Aeronautics and Space Administration Washington, D.C. 20546	14. Sponsoring Agency Code: RTOP 505-43-01

15. Supplementary Notes

Technical Monitor: David G. Koenig, Mail Stop 247-1, NASA Ames Research Center, Moffett Field, Ca 94035. Phone (415) 965-5047 FTS 448-5047

16. Abstract

A trade study to select the best main engine candidate for an advanced STOVL aircraft flight demonstrator was conducted. The aircraft uses ejectors powered by engine bypass flow together with vectored core exhaust to achieve vertical thrust capability. Bypass flow and core flow are exhausted through separate nozzles during wingborne flight.

Six present day or near term turbofan engines were examined for suitability for this aircraft concept. Fan pressure ratio, thrust split between bypass and core flow, and total thrust level were the significant parameters used to compare engines. One of the six candidate engines was selected for the flight demonstrator configuration.

Several smaller propulsion studies related to this aircraft concept were also conducted. A preliminary candidate for the aircraft Reaction Control System for hover attitude control was selected. A mathematical model of transfer of bypass thrust from ejectors to aft-directed nozzle during the transition to wingborne flight was developed. An equation used to predict ejector secondary air flow rate and ram drag was also derived.

Additional topics discussed include nozzle area control, ejector to engine inlet reingestion, bypass/core thrust split variation, and gyroscopic behavior during hover.

17. Key Words (Suggested by Author(s))	18. Distribution Statement
VSTOL STOVL EJECTORS THRUST AUGMENTATION GAS TURBINES JET ENGINES REACTION CONTROL SYSTEMS PROPULSION	FEDD Subject Category -01

19. Security Classif. (of this report)	20. Security Classif. (of this page)	21. No. of Pages	22. Price*
Unclassified	Unclassified	79	

Available: NASA Industrial Applications Centers

End of Document